Article

Cell

The *C. elegans* Taste Receptor Homolog LITE-1 Is a Photoreceptor

Graphical Abstract

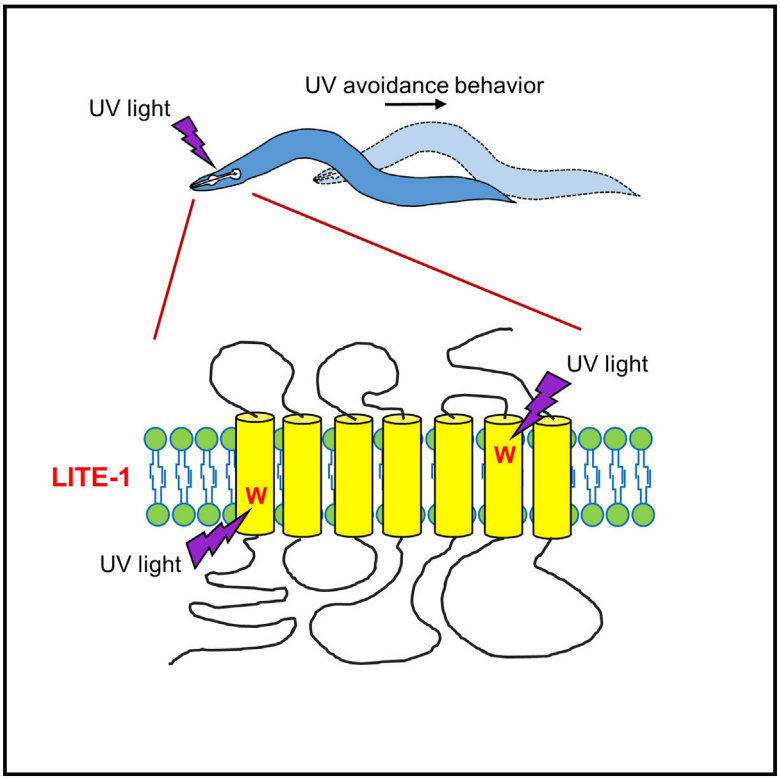

Authors

Jianke Gong, Yiyuan Yuan, Alex Ward, ..., Zhaoyang Feng, Jianfeng Liu, X.Z. Shawn Xu

Correspondence

jfliu@mail.hust.edu.cn (J.L.), shawnxu@umich.edu (X.Z.S.X.)

In Brief

A taste receptor homolog absorbs UV light and mediates avoidance behavior in *C. elegans* in response to light exposure.

Highlights

- LITE-1, a taste receptor homolog, is a bona fide photoreceptor that senses UV light
- LITE-1 has a high efficiency of photon capturing
- Photoabsorption by LITE-1 relies on its conformation and requires two Trp residues
- Introducing such a Trp residue into a related protein promotes photosensitivity

Gong et al., 2016, Cell *167*, 1252–1263
November 17, 2016
http://dx.doi.org/10.1016/j.cell.2016.10.053

CellPress

Cell

Article

The *C. elegans* Taste Receptor Homolog LITE-1 Is a Photoreceptor

Jianke Gong,[1,2] Yiyuan Yuan,[2,4] Alex Ward,[2] Lijun Kang,[2,5] Bi Zhang,[1,2] Zhiping Wu,[3] Junmin Peng,[3] Zhaoyang Feng,[4] Jianfeng Liu,[1,*] and X.Z. Shawn Xu[2,6,*]

[1]College of Life Science and Technology, Collaborative Innovation Center for Brain Science, and Key Laboratory of Molecular Biophysics of MOE, Huazhong University of Science and Technology, Wuhan, Hubei 430074, China

[2]Life Sciences Institute and Department of Molecular and Integrative Physiology, University of Michigan, Ann Arbor, MI 48109, USA

[3]Departments of Structural Biology and Developmental Neurobiology, St. Jude Children's Research Hospital, Memphis, TN 38105, USA

[4]Department of Pharmacology, Case Western Reserve University, Cleveland, OH 44106, USA

[5]Present address: Institute of Neuroscience, Zhejiang University School of Medicine, Hangzhou, Zhejiang 310058, China

[6]Lead Contact

*Correspondence: jfliu@mail.hust.edu.cn (J.L.), shawnxu@umich.edu (X.Z.S.X.)

http://dx.doi.org/10.1016/j.cell.2016.10.053

SUMMARY

Many animal tissues/cells are photosensitive, yet only two types of photoreceptors (i.e., opsins and cryptochromes) have been discovered in metazoans. The question arises as to whether unknown types of photoreceptors exist in the animal kingdom. LITE-1, a seven-transmembrane gustatory receptor (GR) homolog, mediates UV-light-induced avoidance behavior in *C. elegans*. However, it is not known whether LITE-1 functions as a chemoreceptor or photoreceptor. Here, we show that LITE-1 directly absorbs both UVA and UVB light with an extinction coefficient 10–100 times that of opsins and cryptochromes, indicating that LITE-1 is highly efficient in capturing photons. Unlike typical photoreceptors employing a prosthetic chromophore to capture photons, LITE-1 strictly depends on its protein conformation for photon absorption. We have further identified two tryptophan residues critical for LITE-1 function. Interestingly, unlike GPCRs, LITE-1 adopts a reversed membrane topology. Thus, LITE-1, a taste receptor homolog, represents a distinct type of photoreceptor in the animal kingdom.

INTRODUCTION

Light sensation is critical for all phyla of life, ranging from bacteria to humans (Wang and Montell, 2007; Yau and Hardie, 2009). Organisms have evolved various types of photoreceptor proteins (hereinafter referred to as photoreceptors) to detect light (Falciatore and Bowler, 2005; Wang and Montell, 2007; Yau and Hardie, 2009). These photoreceptors show different spectral properties, with some sensing blue and others detecting green and red, covering a wide spectrum of light (Falciatore and Bowler, 2005; Wang and Montell, 2007; Yau and Hardie, 2009). Photoreceptors are typically composed of two moieties: a host protein and a prosthetic chromophore (e.g., retinal), the latter of which is responsible for light absorption (Wang and Montell, 2007; Yau and Hardie, 2009). In addition to image-forming photoreceptor cells in the retina, a growing list of non-image-forming photosensitive cells/tissues has been identified in a wide range of animal species (Wang and Montell, 2007; Yau and Hardie, 2009). For example, a subset of ganglion and horizontal cells in the vertebrate retina are photosensitive (Yau and Hardie, 2009). Photosensitive cells are also found in the skin (e.g., keratinocytes and melanocytes) of mammals, the pupil of most vertebrates, the pineal of non-mammalian vertebrates, the hypothalamus of birds, and the body surface of insects (Bellono et al., 2013; Foster and Soni, 1998; Moore et al., 2013; Xiang et al., 2010; Yau and Hardie, 2009). However, in contrast to microbes and plants, which express many types of photoreceptors, only two such groups of proteins have been identified in the animal kingdom: opsins and cryptochromes (Wang and Montell, 2007; Yau and Hardie, 2009). The question thus arises as to whether unknown types of photoreceptors exist in metazoans.

The nematode *C. elegans* detects and responds to a wide variety of sensory cues such as mechanical forces (e.g., touch and stretch), chemicals (e.g., odorants and tastants), and temperature, representing a popular genetic model organism for the study of sensory perception (de Bono and Maricq, 2005). Despite the lack of eyes, *C. elegans* also responds to light (Edwards et al., 2008; Ward et al., 2008). Specifically, short wavelengths of light, particularly UV light, induce avoidance behavior (negative phototaxis) in *C. elegans*, which is mediated by a group of photosensory neurons, providing a protective mechanism for the worm to avoid lethal doses of UV in the sunlight (Liu et al., 2010; Ward et al., 2008). LITE-1, a member of the invertebrate seven-transmembrane (7-TM) gustatory receptor (GR) family, is required for UV-light-induced avoidance behavior (Edwards et al., 2008; Liu et al., 2010). Ectopic expression of LITE-1 can confer photo-sensitivity to photo-insensitive cells (Edwards et al., 2008; Liu et al., 2010). Despite such indirect evidence suggesting LITE-1 as a candidate photoreceptor, other possibilities remain. For example, unlike long wavelengths of light, UV illumination produces reactive oxygen species (ROS) such as H_2O_2, which in turn can evoke an avoidance behavioral response similar to that induced by UV light (Bhatla and Horvitz, 2015). Given that LITE-1 is a member of the gustatory receptor (GR) family, it has thus been suggested that LITE-1 may function

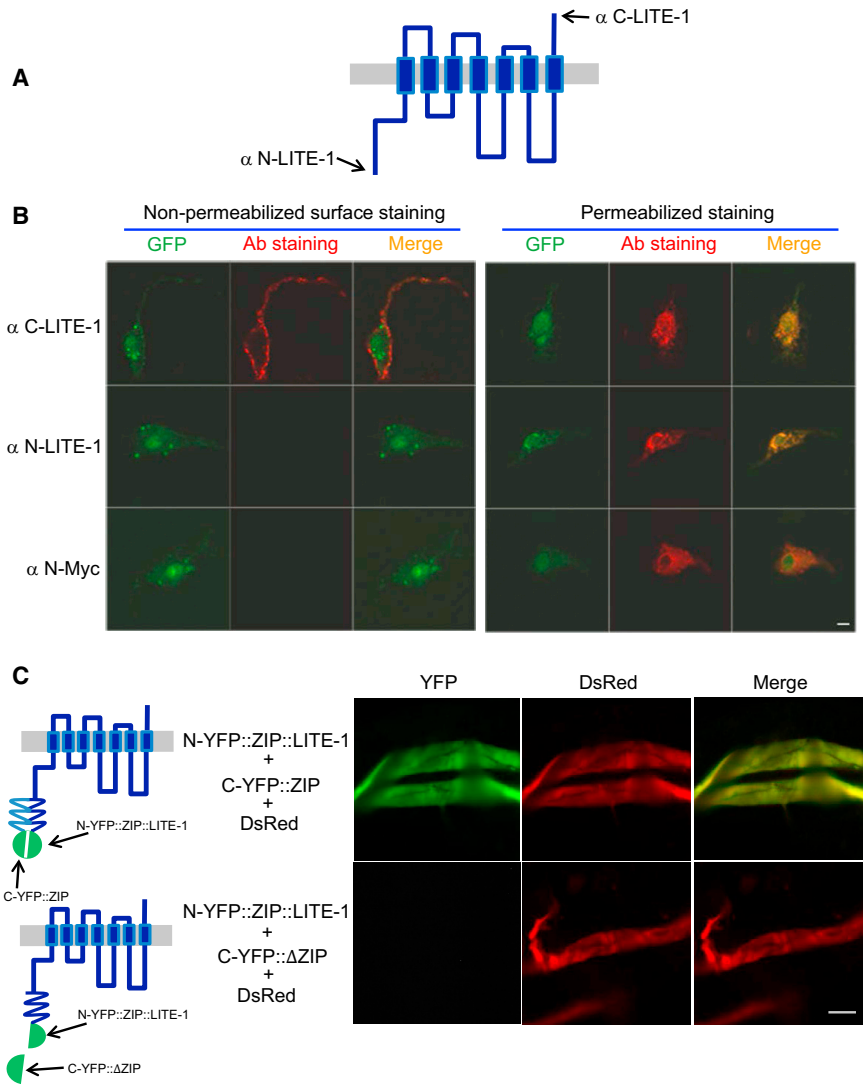

Figure 1. LITE-1 Adopts an Unusual Membrane Topology, with Its C Terminus Facing Extracellularly and N Terminus Located Intracellularly

(A) A schematic of LITE-1 membrane topology. Antibodies were raised against the N-terminal (αN-LITE-1) and C-terminal (αC-LITE-1) peptide (15 aa) of the LITE-1 long isoform.

(B) LITE-1 displays a distinct membrane topology, with its C terminus facing extracellularly and it N terminus located in the cytoplasm. Shown are confocal images from immunofluorescence staining. LITE-1 was co-expressed with GFP as a transgene in muscles under the *myo-3* promoter. Staining was performed on primary cultured cells under non-permeabilizing conditions for surface staining or under permeablizing conditions to stain the entire cell. αN-LITE-1 and αC-LITE-1 detect the N- and C-terminal end of LITE-1, respectively. αN-Myc stains the Myc tag fused to the N-terminal end of LITE-1. See Figure S1 for controls. Scale bar, 2 μm.

(C) BiFC images showing that the N terminus of LITE-1 is located in the cytoplasm. Shown on the left are schematics describing the design of the BiFC approach. Shown on the right are fluorescence images. N-YFP::ZIP::LITE-1 was expressed as a transgene in muscles using the *myo-3* promoter. C-YFP::ZIP (or C-YFP::ΔZIP that lacks a zipper domain) and DsRed were co-expressed as a separate transgene in muscles using the same promoter. Two transgenes were crossed together to examine reconstitution of YFP fluorescence in muscles. Only if the N terminus of LITE-1 is located intracellularly would one be able to detect YFP fluorescence. Muscles were acutely dissected out from transgenic worms using a protocol described previously (Liu et al., 2013). Scale bar, 100 μm.

Also see Figure S1.

as a chemoreceptor (Yau and Hardie, 2009). In this case, LITE-1 would sense light-produced chemicals, but not light per se.

To address this conundrum, here we purified LITE-1 protein from worm lysate and found that it directly absorbs UVA and UVB light. This property of LITE-1, together with its capacity in producing light-evoked functional outputs in vivo, indicates that LITE-1 is a photoreceptor. LITE-1 bears a number of unique features that distinguish it from other photoreceptors. These include an exceptionally high efficiency in photoabsorption, an ability to sense both UVA and UVB light, a strict dependence on conformation for photoabsorption, a strong resistance to bleaching by UV light, and a reversed membrane topology compared to opsins. These results identify LITE-1, a taste receptor homolog, as a unique photoreceptor, with features not seen in any known photoreceptors. Thus, novel types of photoreceptors are present in the animal kingdom. Furthermore, we identified two tryptophan residues in LITE-1 that are critical for photoabsorption. Remarkably, introducing such a tryptophan residue into another GR family member promotes photosensitivity, opening up the intriguing prospect that it might be possible to genetically engineer new photoreceptors.

RESULTS

LITE-1 Adopts a Membrane Topology Opposite to Conventional 7-TM Receptors

As a first step, we considered whether LITE-1 is related to any known photoreceptors. LITE-1 is predicted to contain 7-TM domains (Figure 1A). The only known 7-TM photoreceptors in metazoans are opsins, but LITE-1 has no significant homology with opsins at the sequence level (Edwards et al., 2008; Liu et al., 2010). As both insect OR (olfactory receptors) and GR (gustatory receptors) members were shown to possess a membrane topology opposite to conventional 7-TM receptors (Benton et al., 2006; Zhang et al., 2011), we thus questioned whether LITE-1 and opsins are even related at the membrane topology level.

To probe the membrane topology of LITE-1, we raised antibodies against the N and C termini of LITE-1 (Figure 1A). Immunostaining with these antibodies did not reveal consistent LITE-1 expression in worm tissues (A.W. and X.Z.S.X., unpublished data), suggesting that LITE-1 is expressed at a very low level in vivo. We therefore generated transgenic animals expressing LITE-1 in muscle cells using a muscle-specific promoter, as LITE-1 can be functionally expressed in these cells at a higher level, though it remains possible that recombinant LITE-1 may not fully preserve all the functional properties of native proteins (Edwards et al., 2008; Liu et al., 2010) (also see below). We found that our LITE-1 antibodies can detect LITE proteins in primary cultured muscle cells (Figure 1B). Surprisingly, the C-terminal end of LITE-1 appears to be extracellular, as antibodies against LITE-1's C terminus can detect LITE-1 when applied extracellularly under non-permeabilizing conditions (Figure 1B). This staining is specific for LITE-1 since no signal was observed in control muscle cells (Figure S1). By contrast, the same protocol failed to detect LITE-1 with antibodies against its N-terminal end, though the protein was clearly expressed in these cells, as shown under permeabilizing conditions (Figure 1B). To provide additional evidence, we fused a Myc tag to the N-terminal end of LITE-1 and obtained the same result (Figure 1B). This suggests that the N-terminal end of LITE-1 is intracellular.

To collect further evidence, we employed the BiFC (bimolecular fluorescence complementation) approach (Hu et al., 2002). In this approach, the N- and C-terminal fragment of YFP is fused to a leucine zipper domain to generate N-YFP::ZIP and C-YFP::ZIP, respectively (Figure 1C). The zipper domains then bring the two YFP fragments together to reconstitute a fluorescent YFP protein (Figure 1C). We attached N-YFP::ZIP to the N terminus of LITE-1 and found that this N-YFP::ZIP::LITE-1 fusion complemented with C-YFP::ZIP to reconstitute YFP fluorescence in live muscle cells acutely dissected from the animal, but not with C-YFP::ΔZIP that lacked the zipper domain (Figure 1C). This observation further demonstrates that the N terminus of LITE-1 is located intracellularly. We conclude that LITE-1 adopts a reversed membrane topology compared to opsins. Thus, LITE-1 does not seem to be closely related to any known photoreceptors at the sequence or structural levels.

Purification of LITE-1 Protein from Worm Lysate

Is LITE-1 a photoreceptor? A lack of clear similarity to known photoreceptors does not necessarily disqualify LITE-1 as a photoreceptor. To address this question, a simple yet definitive approach is to examine whether purified LITE-1 protein can capture photons by spectrophotometry (Wang and Montell, 2007; Yau and Hardie, 2009). All known photoreceptors were verified by this approach (Figure 2I). To this end, we searched for an expression system that would allow us to purify a sufficient amount of LITE-1 protein for spectrophotometric analysis. Muscle cells thus came to our attention, as they constitute a major mass of worm tissues and have been successfully utilized as a heterologous system to functionally express receptors and channels (Salom et al., 2012; Wang et al., 2012). Importantly, it has been shown that LITE-1 can be functionally expressed in muscles, as its expression can confer photo-sensitivity to these otherwise photo-insensitive cells (Edwards et al., 2008; Liu et al., 2010), though it remains unclear whether such photosensitivity results from light or light-produced chemicals. Indeed, as previously reported (Edwards et al., 2008; Liu et al., 2010), UV light can induce the contraction of body-wall muscles ectopically expressing LITE-1, leading to body paralysis (Figures 2A and S2 and Movies S1 and S2). To provide more direct and quantitative evidence, we recorded the response of muscle cells to UV light by calcium imaging using the genetically encoded calcium sensor RCaMP. We found that UV illumination induced robust calcium transients in muscle cells ectopically expressing LITE-1, but not in control muscle cells (Figures 2B–2D). These experiments show that LITE-1 was functionally expressed in muscle cells. They also show that LITE-1 can indeed confer photo-sensitivity to photo-insensitive cells, demonstrating that it can be potentially used as an optogenetic tool.

Since our LITE-1 antibodies are not suitable for affinity purification, we then tested a number of monoclonal antibodies against small affinity tags such as Myc, FLAG, and 1D4 and found that 1D4 antibody worked most efficiently. Using this antibody, we were able to affinity-purify LITE-1, a membrane protein, to homogeneity, as determined by SDS-PAGE followed by Coomassie staining (Figure 2E) and by western blot (Figure 2F). This result was also verified by silver staining (data not shown).

Purified LITE-1 Protein Absorbs Photons

By subjecting purified LITE-1 protein to spectrophotometric analysis, we found that it exhibited strong absorption of UV light, with two absorbance peaks at 280 and 320 nm (Figure 2G). Thus, LITE-1 can capture both UVB and UVA light (WHO definition of UVB: 280–315 nm; UVA: 315–400 nm). As a comparison, at the same concentration (0.4 μM), BSA showed no such absorption (Figure 2G). In addition, bacterial rhodopsin (bRho), which is a commercial product obtained from Sigma Co., exhibited minimal absorption at its signature peak 568 nm (Figure 2H). Only at 10× concentration (4 μM) were we able to detect modest light absorption in bacterial rhodopsin (bRho), which was still much weaker than that found in LITE-1 (Figure 2H). It should be noted that, though bRho exhibited weaker photoabsorption compared to LITE-1, its extinction coefficient (62,000 in Figure 2H versus 63,000 in Figure 2I), as well as its spectral properties, were both in line with those reported in literature (Figures 2H and 2I), indicating that the quality of bRho samples was reliable. The extinction coefficient of both absorbance peaks of LITE-1 is $> 10^6\ M^{-1}cm^{-1}$, which is 10–100 times that of all known photoreceptors (Figure 2I). Thus, LITE-1 has a high efficiency in capturing photons.

To make a more direct comparison, we purified bovine rhodopsin (Rho) ectopically expressed in worm muscles (Salom et al., 2012) and did so side by side with LITE-1 under the same conditions (Figures S3A and S3B). Compared to LITE-1, purified bovine rhodopsin (Rho) also showed much weaker photoabsorption at its signature peak (Figures S3C and S3D), providing additional evidence demonstrating that LITE-1 is highly efficient in capturing photons. The relatively weak photoabsorption by bovine rhodopsin (Rho) was not because our purified Rho samples were of low quality, as the extinction coefficient of the purified Rho was in fact very similar to that reported in literature (Figure S3D versus Figure 2I). In addition, the signature

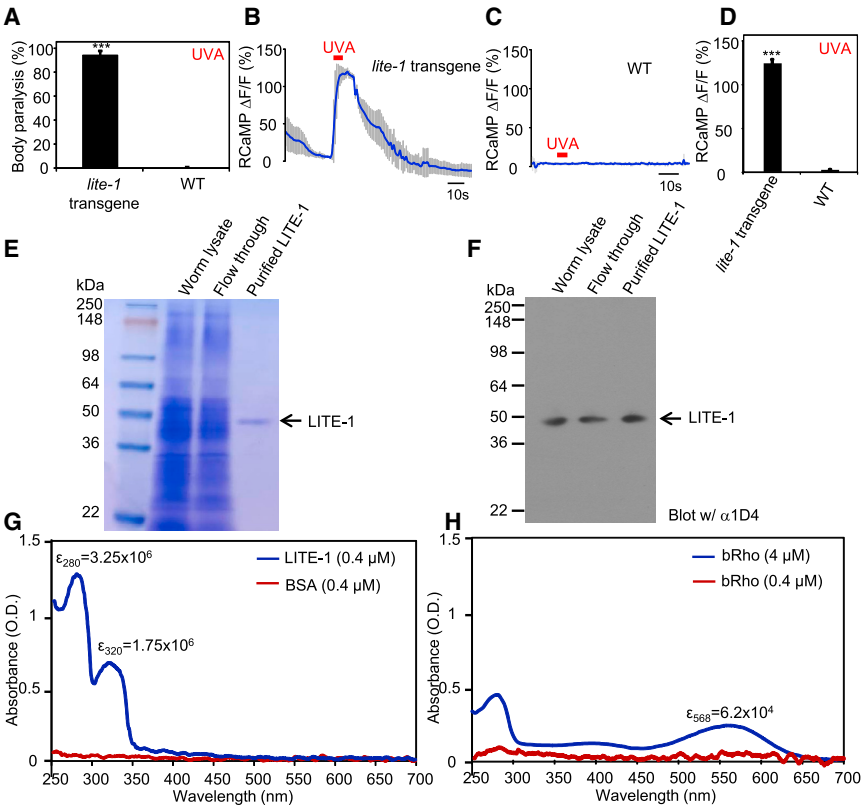

I

Photoreceptor		Wavelength (nm)	Extinction coefficient ($M^{-1}cm^{-1}$)	Species
LITE-1		280	3,760,000±597,000	*C. elegans*
		320	2,240,000±696,000	
Cyptochrome		450	36,000	*Drosophila*
Opsins	Bacterial rhodopsin	568	63,000	*Halobacterium*
	Rhodopsin	500	41,200	*Bovinae*
	Melanopsin	467	33,000	*Mus musculus*
	UV opsin	357	41,760	*Mus musculus*
	Blue opsin	425	39,400	*Xenopus laevis*
	Green opsin	510	40,800	*G. gallus*
	Red opsin	560	47,200	*G. gallus*

Figure 2. LITE-1 Absorbs UVA and UVB Light, and Ectopic Expression of LITE-1 Confers Photo-Sensitivity to Photo-Insensitive Cells

(A) Transgenic expression of LITE-1 in muscle cells confers photosensitivity shown by behavioral assays. LITE-1 was expressed as a transgene in muscle cells under the *myo-3* promoter. WT (wild-type) and LITE-1 transgenic worms were exposed to a 20 s pulse of UVA light (350 ± 20 nm, 0.8 mW/mm^2). Animals showing muscle contraction-induced paralysis during light illumination were scored positive. n = 20. Error bars represent SEM. ***$p < 0.00001$ (ANOVA with Bonferroni test).

(B–D) Transgenic expression of LITE-1 in muscle cells confers photosensitivity shown by calcium imaging. RCaMP was expressed as a transgene in muscle cells under the *myo-3* promoter. The peak percentage change in the intensity of RCaMP fluorescence (ΔF/F) was quantified. A 5 s pulse of UVA light (340 ± 20 nm, 0.7 mW/mm^2) was applied to muscles to elicit calcium transients. Shades along the traces in (B) and (C) represent SEM. (D) Bar graph. n ≥ 7. *$p < 0.0001$ (Student's *t* test).

(E and F) Purification of LITE-1. Worm lysate, flow through, and purified LITE-1 were loaded. Shown in (E) is an SDS-PAGE gel stained with Coomassie blue. Shown in (F) is a western blot probed with anti-1D4 that recognizes the 1D4 tag attached to the C-terminal end of LITE-1. The amount of each sample loaded in (F) was one-tenth of that in (E). Samples for SDS-PAGE and western were prepared at room temperature under non-reducing conditions (free of β-ME and DTT) to avoid aggregation of LITE-1.

(G) LITE-1 shows strong absorption of UVA and UVB light, while BSA does not. The same concentration of purified LITE-1 and BSA (0.4 μM) was subjected to UV-visible spectrophotometric analysis. The extinction coefficient (ε) for both peaks of LITE-1 was noted. Unit: $M^{-1}cm^{-1}$. Note: these numbers only represent the LITE-1 sample shown here and those in Figure 3, as they were from the same batch of purification. See (I) for averaged data for LITE-1 from different batches of purification.

(H) Bacterial rhodopsin (bRho) shows much weaker absorption of light compared to LITE-1. The results from low and high concentrations of bRho were shown. bRho was purchased from Sigma.

(I) LITE-1 is far more efficient in photon absorption than cryptochromes and opsins. The extinction coefficients for LITE-1 were averaged from samples from seven independent purifications. "±" represents SEM. The numbers for cryptochromes and opsins were from published literature: cryptochrome (Thompson and Sancar, 2002), bacterial rhodopsin (Oesterhelt and Hess, 1973), rhodopsin (Okano et al., 1992), melanopsin (Matsuyama et al., 2012), UV opsin (Insinna et al., 2012), blue opsin (Vought et al., 1999), green opsin, and red opsin (Kolesnikov et al., 2014).

See also Figures S2 and S3 and Movies S1 and S2.

absorbance peak of the purified Rho was 500 nm, which was identical to that published in literature (Figure S3D versus Figure 2I). This set of control experiments also validated our experimental system, including protein expression, purification, concentration determination, and spectral analysis.

In another control experiment, we purified mammalian adenosine A_{2A} receptor ($A_{2A}R$) ectopically expressed in worm muscles (Salom et al., 2012) (Figures S3A and S3B). Like LITE-1 and opsins, $A_{2A}R$ is also a 7-TM receptor but is not expected to be photosensitive. Indeed, we found that, as predicted, this receptor did not absorb light when purified and tested side by side with LITE-1 and Rho (Figure S3C). Thus, multiple control experiments support that LITE-1 absorbs photons and does so at a high efficiency. This property of LITE-1, together with its capacity in producing various light-induced functional outputs [e.g., light-induced muscle contraction and calcium transients and avoidance behavior ([Figures 2A–2D and S2 and Movies S1 and S2]), indicates that LITE-1 is a photoreceptor. LITE-1 is also the only photoreceptor that shows strong absorption of both UVA and UVB light.

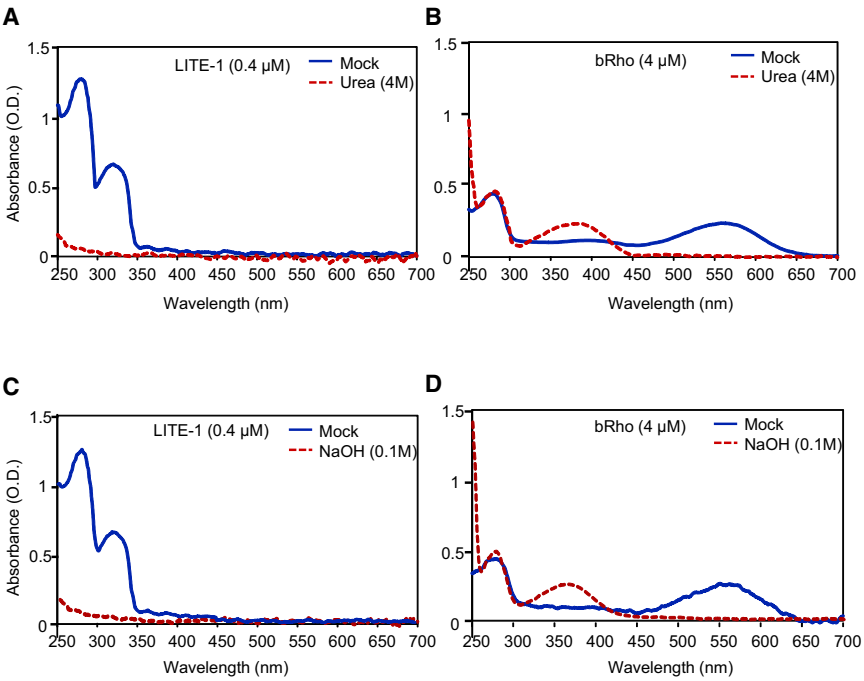

Figure 3. Photoabsorption by LITE-1 Relies on Its Conformation

(A) Denaturing LITE-1 with urea abolishes its photoabsorption. Shown are spectral data for mock- and urea-treated LITE-1. LITE-1 was treated with urea (4 M) for 5 min at room temperature prior to spectral analysis.

(B) Denaturing bacterial rhodopsin (bRho) with urea does not eliminate its photoabsorption. Urea treatment shifts bRho's 568 nm absorbance peak to 370 nm. bRho was treated with urea (4 M) for 5 min at room temperature prior to spectral analysis.

(C) Denaturing LITE-1 with NaOH abolishes its photoabsorption. LITE-1 was treated with NaOH (0.1 M) for 5 min at room temperature prior to spectral analysis.

(D) Denaturing bacterial rhodopsin (bRho) with NaOH does not eliminate its photoabsorption. NaOH treatment shifts bRho's 568 nm absorbance peak to 370 nm. bRho was treated with NaOH (0.1 M) for 5 min at room temperature prior to spectral analysis.

LITE-1 concentration: 0.4 μM. bRho concentration: 4 μM.

See also Figure S4.

LITE-1 Strictly Depends on Its Conformation for Photoabsorption

We next sought to characterize the photoabsorption of LITE-1. A photoreceptor is usually composed of two moieties: a host protein and a prosthetic chromophore (Falciatore and Bowler, 2005; Wang and Montell, 2007; Yau and Hardie, 2009). The spectral properties of a photoreceptor are certainly affected by the host protein. However, the absolute ability of a photoreceptor to absorb light does not rely on the host protein, as light absorption is mediated by the chromophore (e.g., retinal, flavin, bilin, and p-coumaric acid) (Falciatore and Bowler, 2005; Marti et al., 1991; Radding and Wald, 1956). Consequently, denaturing a photoreceptor usually shifts its absorbance peaks to different wavelengths but does not eliminate them, as they are mediated by the associated chromophore (Dutta et al., 2010; Hagins, 1973; Hubbard, 1969; Maglova et al., 1989). This, surprisingly, does not appear to be the case for LITE-1. Denaturing LITE-1 with urea abolished the light absorption by LITE-1, eliminating both the 280 and 320 nm peaks (Figure 3A). As a comparison, the same urea treatment failed to abolish the light absorption by bacterial rhodopsin (bRho) but instead shifted its absorbance peak from 568 nm to 370 nm (Figure 3B), the latter of which is the signature peak of free retinal, the chromophore of bRho (Sperling and Rafferty, 1969). A similar phenomenon was observed with our purified bovine rhodopsin (Rho) (Figures S3E and S3F). It is notable that the 280 nm peak of denatured bRho remained unchanged (Figure 3B), consistent with the notion that this peak was mediated by the intrinsic light absorption by tryptophan residues of the bRho protein. This peak was not that distinct in denatured LITE-1 in Figure 3A since the concentration of LITE-1 used was one-tenth that of bRho. We also treated LITE-1 using other denaturing agents such as NaOH and observed a similar phenomenon (Figures 3C and 3D). These observations demonstrate that, unlike typical photoreceptors, LITE-1 strictly depends on its conformation for photoabsorption.

We also tested H_2O_2. Interestingly, H_2O_2 treatment abolished LITE-1's photoabsorption (Figure S4A). As an oxidizing agent, H_2O_2 can damage the function of proteins, lipids, and nucleic acids (Fridovich, 2013). Oxidization of LITE-1 may affect the conformation of LITE-1, which is required for its absorption of light. Similarly, H_2O_2 treatment also destroyed the spectral fingerprint of bRho by shifting its absorbance peak from 568 to 370 nm (Figure S4B). Thus, H_2O_2 appears to inhibit the photoabsorption of both LITE-1 and bRho in vitro. Nevertheless, as it is difficult to estimate the endogenous concentration of H_2O_2, whether and how H_2O_2 affects LITE-1 function in vivo remains to be determined.

Genetic Screens Identify Residues Critical for LITE-1 Function

To obtain a better understanding of LITE-1 photoabsorption, we attempted to identify residues critical for LITE-1 function. In a genetic screen for mutant animals defective in UV-light-induced avoidance behavior, we isolated several *lite-1* mutant alleles (Liu et al., 2010). We hypothesized that mutations in transmembrane domains are more likely to affect the photoabsorption of LITE-1 rather than its coupling to downstream signaling molecules. Two mutants, *lite-1*(*xu8*) and *lite-1*(*xu10*), thus came to our attention, as the residues mutated (A332V and S226F, respectively) reside in putative transmembrane domains (Figure 7I). The objective was to purify these mutant forms of LITE-1 protein and then characterize their photoabsorption in vitro. We first tested their role in vivo and found that, as

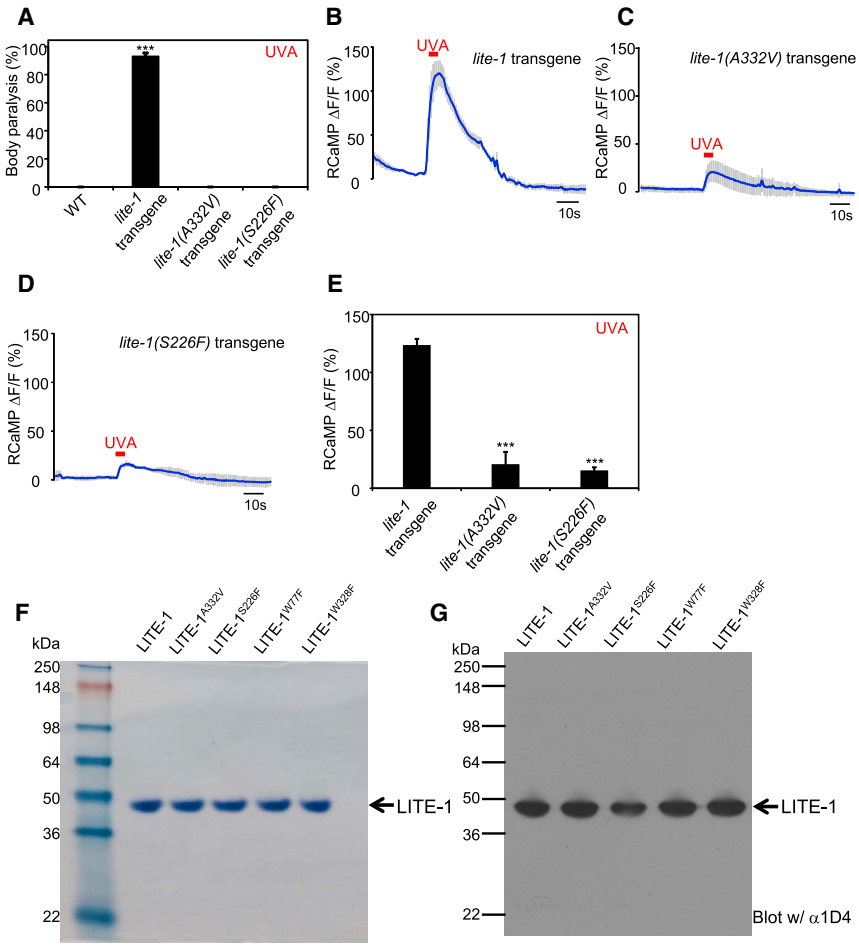

Figure 4. Residues S226 and A332 in LITE-1 Are Critical for Its Sensitivity to UVA Light In Vivo

(A) S226F and A332V mutations disrupt the function of LITE-1 in vivo shown by behavioral assays. LITE-1 harboring S226F or A332V was expressed as a transgene in muscles under the *myo-3* promoter. WT (wild-type) and transgenic worms were exposed to a 20 s pulse of UVA light (350 ± 20 nm, 0.8 mW/mm^2). Animals showing muscle contraction-induced paralysis during light illumination were scored positive. Some genotypes had all data points as zero, and thus no statistical analysis was performed on them. n = 20. Error bars: SEM. ***p < 0.00001 (ANOVA with Bonferroni test).

(B–E) S226F and A332V mutations disrupt the function of LITE-1 in vivo, shown by calcium imaging. The experiments were done as described in Figure 2B. A 5 s pulse of UVA light (340 ± 20 nm, 0.7 mW/mm^2) was applied to muscles to elicit calcium transients. Shades along the traces in (B–D) represent SEM. (E) Bar graph. n ≥ 7. ***p < 0.00001 (ANOVA with Bonferroni test).

(F and G) Purification of mutant forms LITE-1. Shown in (F) is an SDS-PAGE gel stained with Coomassie blue. Shown in (G) is a western blot probed with anti-1D4 that recognizes the 1D4 tag attached to the C terminus of LITE-1 variants. The amount of each sample loaded in (G) was 1/10 of that in (F). Samples for SDS-PAGE and western were prepared at room temperature under non-reducing conditions (free of β-ME and DTT) to avoid aggregation of LITE-1.

See also Figure S5.

expected, A332V and S226F mutations disrupted LITE-1 function in vivo. Specifically, worms ectopically expressing LITE-1 harboring either mutation were no longer sensitive to UVA light in behavioral assays (Figures 4A and S5A). In addition, these two point mutations nearly abolished UVA-light-evoked calcium transients in muscle cells ectopically expressing LITE-1 (Figures 4B–4E). We successfully purified LITE-1^{A332V} and LITE-1^{S226F} proteins to homogeneity (Figures 4F and 4G). LITE-1^{A332V} and LITE-1^{S226F} displayed an absorbance spectrum distinct from wild-type LITE-1: they both lost the 320 nm peak but retained normal absorption at 280 nm (Figures 5A and 5B). Thus, the two mutations disrupted LITE-1's absorption of UVA but not UVB light. This is consistent with the fact that our genetic screen was targeted for isolating mutants defective in responding to UVA but not UVB light, since the optical system of the microscope used to evoke and assay phototaxis behavior did not transmit UVB light (Liu et al., 2010).

Given that LITE-1^{A332V} and LITE-1^{S226F} proteins retained normal absorption of UVB light in vitro, one would predict that these two mutant forms of LITE-1 shall preserve the sensitivity to UVB light in vivo. To test this idea, we set up an optical path through which UV light was directed to the worm directly. Indeed, though transgenic worms expressing these two mutant forms of LITE-1 were insensitive to UVA light (Figures 4A and S5A), they were nevertheless sensitive to UVB light (Figures 5C and S5B). In addition, as was the case with wild-type LITE-1, UVB light also induced robust calcium transients in muscle cells ectopically expressing these two mutant forms of LITE-1 (Figures 5D–5H). These results are in line with the data from spectral analysis (Figures 5A and 5B). Thus, it appears that the absorption of UVA and UVB light by LITE-1 can be separated, providing further evidence demonstrating the specificity of LITE-1 photoabsorption.

LITE-1 Absorption of UVB but Not UVA Light Shows Resistance to Photobleaching

Prolonged light illumination bleaches photoreceptors (Wang and Montell, 2007; Yau and Hardie, 2009). We tested this property of LITE-1 and found that pre-exposure to UV light can readily bleach LITE-1's ability to absorb UVA light by eliminating its 320 nm peak (Figure 5I). Surprisingly, such treatment spared the 280 nm peak (Figure 5I), indicating that the ability for LITE-1 to capture UVB light was more stable and relatively resistant to photobleaching. This experiment reveals an additional feature that distinguishes LITE-1 absorption of UVA and UVB light.

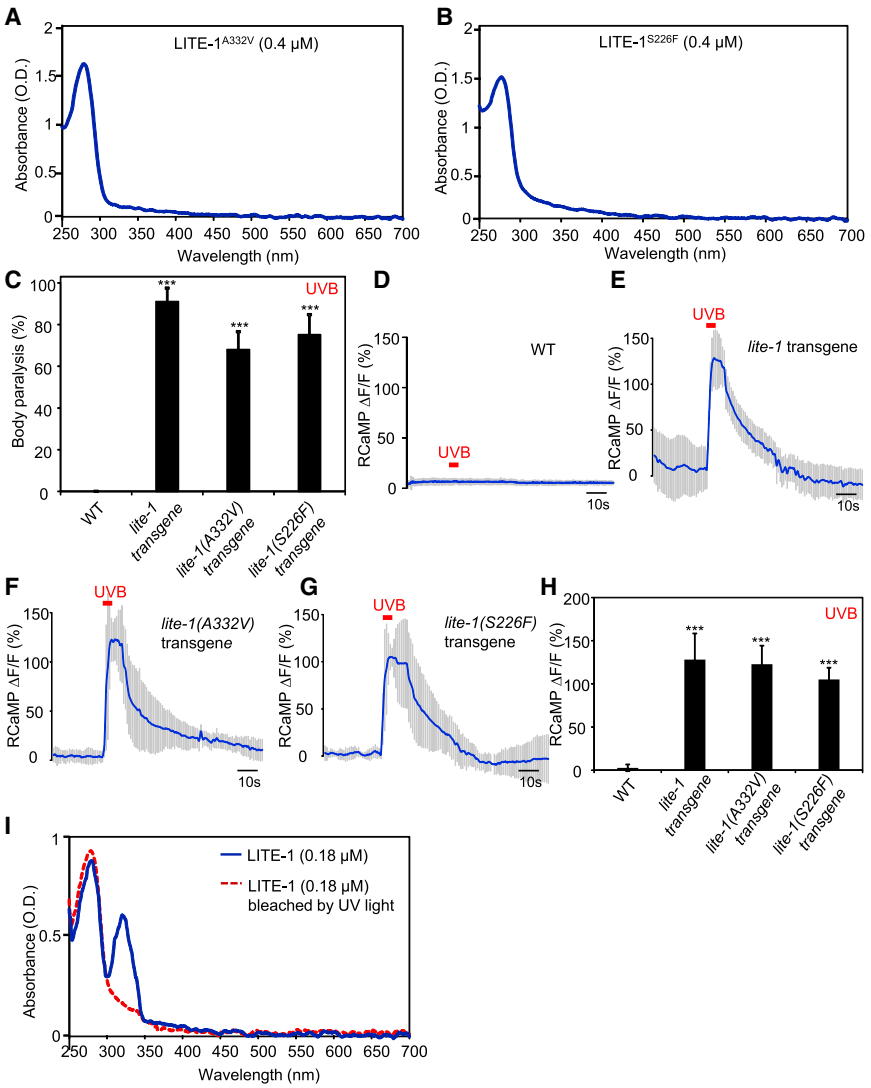

Figure 5. Residues S226 and A332 in LITE-1 Are Required for Its Absorption of UVA but Not UVB Light In Vitro

(A and B) S226F and A332V mutations disrupt LITE-1's absorption of UVA but not UVB light in vitro. The extinction coefficient at 280 nm for LITE-1^{A332V} and LITE-1^{226F} is: 4.0 × 10^6 M^{-1}cm^{-1} and 3.75 × 10^6 M^{-1}cm^{-1}, respectively, which are similar to wild-type LITE-1 (Figure 2I).

(C) S226F and A332V mutations do not disrupt the sensitivity of LITE-1 to UVB light in vivo, shown by behavioral assays. LITE-1 harboring S226F or A332V was expressed as a transgene in muscle cells under the *myo-3* promoter. WT (wild-type) and transgenic worms were exposed to a 20 s pulse of UVB light (280 ± 10 nm, 0.03 mW/mm^2). Animals showing muscle contraction-induced paralysis during light illumination were scored positive. n = 20. Error bars represent SEM. ***p < 0.00001 (ANOVA with Bonferroni test).

(D–H) S226F and A332V mutations do not disrupt the sensitivity of LITE-1 to UVB light in vivo, shown by calcium imaging. The experiments were done as described in Figure 2B. A 5 s pulse of UVB light (280 ± 10 nm, 0.02 mW/mm^2) was applied to muscles to elicit calcium transients. Shades along the traces in (D–G) represent SEM (H) Bar graph. n ≥ 10. ***p < 0.00001 (ANOVA with Bonferroni test).

(I) LITE-1 absorption of UVB but not UVA light shows resistance to photobleaching. LITE-1 was pre-exposed to UV light for 5 min (17 μW/mm^2, 302 nm) at room temperature prior to spectrophotometric analysis. Pre-exposure to UV light for 30 min still did not notably affect the UVB photoabsorption. The photoabsorption at 280 nm was eventually lost after 1 hr of pre-exposure, probably because LITE-1 was denatured. As a direct comparison, bRho, when tested under the same condition, showed photobleaching of its 568 nm peak after pre-exposure to ambient light for <5 min, and such photobleaching became complete at 10 min. See also Figure S5.

Two Tryptophan Residues Are Required for LITE-1 Function

Our success in identifying residues critical for LITE-1's absorption of UVA light encouraged us to explore what may underlie its absorption of UVB light. Tryptophan residues show intrinsic absorption of UVB light, peaking at 280 nm. It is also known that light absorption by tryptophan is quite resistant to photobleaching (Wu et al., 2008). These two features together led us to question whether tryptophan residues in LITE-1 play a role in mediating its absorption of UVB light. Six tryptophan residues are found in LITE-1 (Figure 7I). However, should any of these tryptophan residues be important for LITE-1 function, they would not be expected to be picked up by our genetic screen, as the mutagen (EMS) used in the screen would typically mutate a tryptophan residue to a stop codon rather than generate a missense mutation.

Therefore, to test the above hypothesis, we mutated each of the six tryptophan residues to alanine through site-directed mutagenesis and expressed the corresponding mutant form of LITE-1 as a transgene in muscle cells. We first examined their function in vivo. Two tryptophan residues, W77 and W328, when mutated to alanine, abolished the sensitivity of LITE-1 to UVA light in vivo in behavioral assays (Figures 6A and S6A), whereas mutating the other four tryptophan residues did not elicit a notable effect (Figure 6A). We obtained a similar result when mutating W77 and W328 to F (phenylalanine) (Figure 6A). Furthermore, the two tryptophan mutations W77F and W328F nearly eliminated UVA-light-induced calcium transients in muscle cells ectopically expressing LITE-1 (Figures 6C–6F). These data identify a critical role for W77 and W328 in LITE-1 function in vivo.

Lastly, we purified the two mutant forms of LITE-1, LITE-1^{W77F} and LITE-1^{W328F}, to homogeneity (Figures 4F and 4G) and examined their photoabsorption in vitro. Strikingly, W77F and W328F mutations not only abolished LITE-1's absorption of UVA light at 320 nm, but also nearly eliminated its absorption of UVB light at

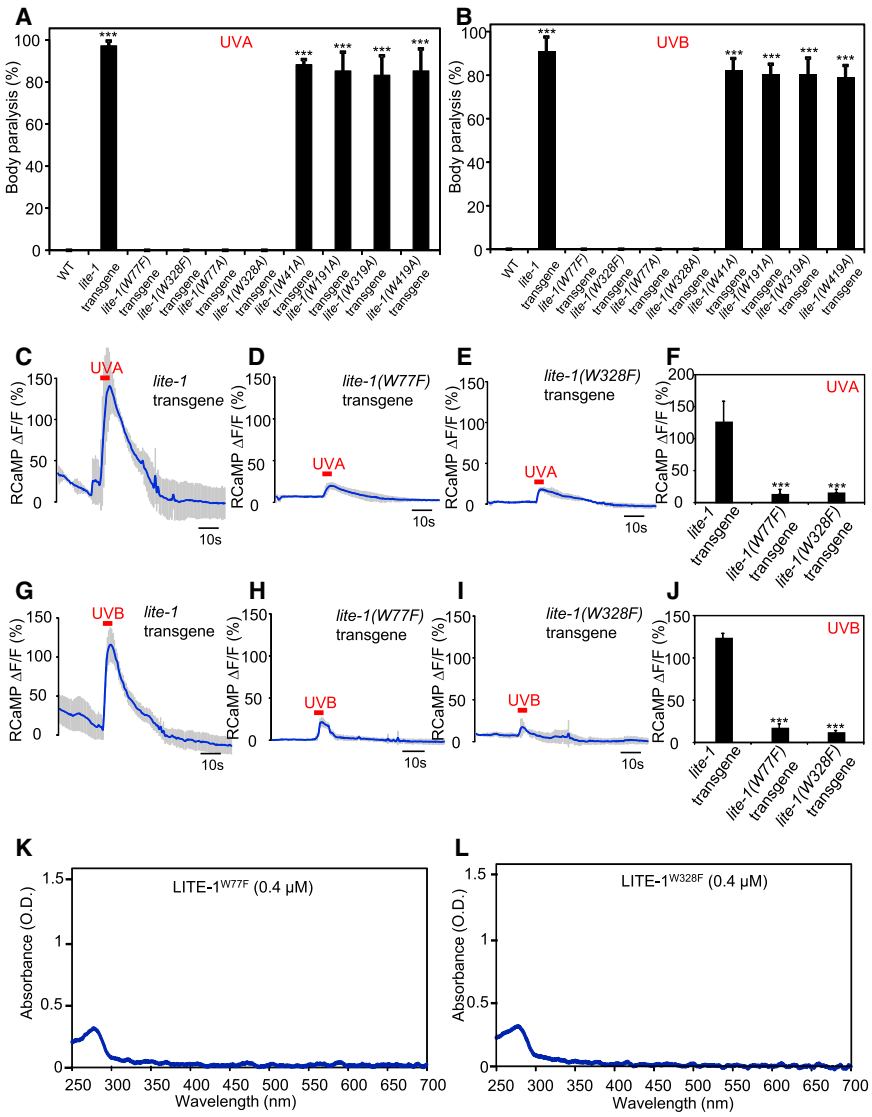

Figure 6. The Two Tryptophan Residues W77 and W328 in LITE-1 Are Required for LITE-1 Function Both In Vivo and In Vitro

(A and B) Mutating W77 and W328 but not the other four W residues disrupts the sensitivity of LITE-1 to both UVA and UVB light in vivo, shown by behavioral assays. LITE-1 variants harboring mutations in each W residue were expressed as a transgene in muscle cells. Wild-type (WT) and transgenic worms were exposed to a 20 s pulse of UVA light (A) or UVB light (B). Animals showing muscle contraction-induced paralysis during light illumination were scored positive. n = 20. Error bars represent SEM. ***p < 0.00001 (ANOVA with Bonferroni test).

(C–F) W77F and W328F mutations disrupt the sensitivity of LITE-1 to UVA light in vivo, shown by calcium imaging. The experiments were done as described in Figure 2B. A 5 s pulse of UVA light (340 ± 20 nm, 0.7 mW/mm^2) was applied to muscles to elicit calcium transients. Shades along the traces in (C–E) represent SEM. (F) Bar graph. n ≥ 6. ***p < 0.00001 (ANOVA with Bonferroni test).

(G–J) W77F and W328F mutations disrupt the sensitivity of LITE-1 to UVB light in vivo, shown by calcium imaging. A 5 s pulse of UVB light (280 ± 10 nm, 0.02 mW/mm^2) was applied to muscles to elicit calcium transients. Shades along the traces in (G–I) represent SEM. (J) Bar graph. n ≥ 10. ***p < 0.00001 (ANOVA with Bonferroni test).

(K and L) W77F and W328F mutations disrupt LITE-1's absorption of both UVA and UVB light in vitro.

See also Figure S6.

280 nm (Figures 6K and 6L). Consistently with this spectral data, we found that these two tryptophan mutations abolished the sensitivity of LITE-1 to UVB light in vivo in behavioral assays (Figures 6B and S6B). In addition, UVB light elicited little if any calcium transients in muscle cells ectopically expressing these two mutant forms of LITE-1 (Figures 6G–6J). The residual calcium response evoked by UVA and UVB light in these muscle cells arose from the other tryptophan residue, as mutating both tryptophan residues eliminated the response (J.G. and X.Z.S.X., unpublished data). Thus, the two tryptophan residues W77 and W328 are critical for LITE-1 function both in vivo and in vitro. These experiments identify key molecular determinants required for LITE-1 function in vivo and in vitro.

Genetic Engineering of Photoreceptors

To provide further evidence supporting a critical role for the two tryptophan residues in mediating photoabsorption, we wondered whether introducing such tryptophan residues into another protein would promote photoabsorption. On the other hand, tryptophan residues alone are unlikely to underpin the high photoabsorption capacity of LITE-1, and other parts of LITE-1 must be involved, which may serve as a "backbone" to support the function of the two tryptophan residues in capturing photons. We thus reasoned that those proteins related to LITE-1, such as other GR genes, may possess such a backbone structure and thereby would have a higher likelihood to be engineered as a photoreceptor. The *C. elegans* GR family contains five members. With the exception of LITE-1, no other GR genes have both tryptophan residues at the corresponding positions (Figure S7A). We noticed that, although GUR-3 is not that similar to LITE-1 at the sequence level (40% sequence identity with LITE-1), it has one tryptophan residue in place, which corresponds to W328 in LITE-1 (Figure S7A). GUR-3 was suggested to function as a chemoreceptor (Bhatla and Horvitz, 2015). Ectopic expression of GUR-3 in muscle cells did not promote their sensitivity to UV light in behavioral assays (Figures 7A, S7B, S7F, and S7G), suggesting that GUR-3 has little or no photosensitivity. Indeed, calcium imaging revealed that UV light only evoked little calcium response in muscle cells ectopically expressing

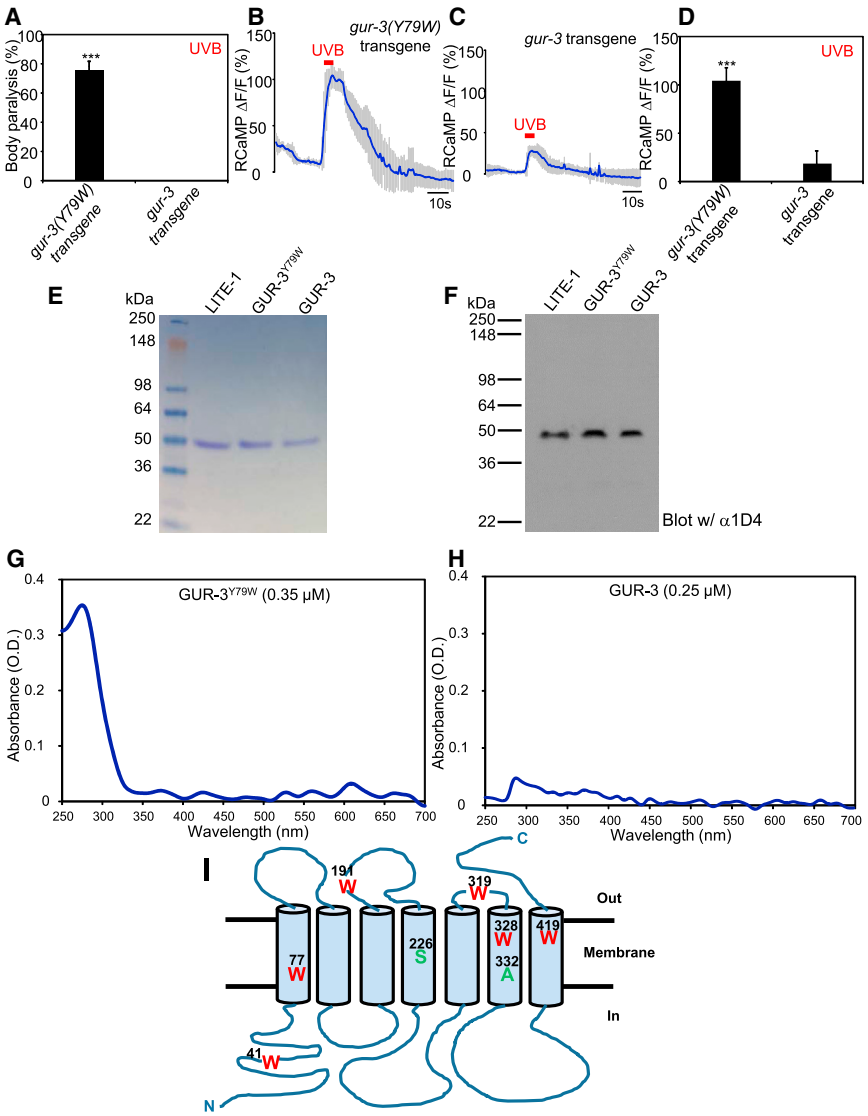

Figure 7. Genetic Engineering of a Photoreceptor by Introducing a Tryptophan Residue into Another GR Family Member, GUR-3

(A) Mutating Y79 to W in GUR-3 promotes photosensitivity in vivo shown by behavioral assays. GUR-3^{Y79W} and GUR-3 were expressed as a transgene in muscle cells. Worms were exposed to a 20 s pulse of UVB light (280 ± 10 nm, 0.03 mW/mm^2), and those showing muscle contraction-induced paralysis during light illumination were scored positive. n = 50. Error bars represent SEM. ***p < 0.00001 (Student's *t* test).

(B–D) Mutating Y79 to W in GUR-3 promotes photosensitivity in vivo, shown by calcium imaging. The experiments were done as described in Figure 2B. A 5 s pulse of UVB light (280 ± 10 nm, 0.02 mW/mm^2) was applied to muscles to elicit calcium transients. Shades along the traces in (B) and (C) represent SEM. (D) Bar graph. n = 20. ***p < 0.00001 (Student's *t* test).

(E and F) Purification of GUR-3^{Y79W} and GUR-3. Shown in (E) is an SDS-PAGE gel stained with Coomassie blue. Shown in (F) is a western blot probed with anti-1D4 that recognizes the 1D4 tag attached to the C terminus of GUR-3^{Y79W} and GUR-3, as well as LITE-1. LITE-1 was purified side by side as a reference. As predicted, GUR-3 showed a slightly larger molecular weight than LITE-1. The amount of each sample loaded in (F) was one-tenth of that in (E). Samples for SDS-PAGE and western were prepared at room temperature under non-reducing conditions (free of β-ME and DTT) to avoid aggregation of LITE-1.

(G and H) Mutating Y79 to W in GUR-3 greatly potentiates the absorption of UVB light (280 nm) in vitro.

(I) A schematic model denoting LITE-1 membrane topology and the position of residues investigated in this study.

See also Figure S7.

GUR-3 (Figures 7C, 7D and S7C–S7E). We then mutated residue Y79 in GUR-3 to W (i.e., GUR-3^{Y79W}), which corresponds to W77 in LITE-1 (Figure S7A). Strikingly, worms ectopically expressing the tryptophan-bearing GUR-3^{Y79W} then became very sensitive to UVB light (Figures 7A and S7G). UVA light was not that effective on these worms (Figures S7B–S7F). This result was expected, as UVA absorption by LITE-1 apparently requires additional key elements such as residues A226 and S332 and perhaps others (Figures 4A–4E). We also examined UVB-light-evoked calcium transients in muscle cells and found that ectopic expression of the tryptophan-bearing GUR-3^{Y79W} greatly potentiated UVB-light-induced calcium response in these cells (Figures 7B–7D). Thus, introducing a tryptophan residue into GUR-3 promotes photosensitivity.

Having characterized the photosensitivity of GUR-3^{Y79W} and GUR-3 in vivo, we then purified both proteins to homogeneity (Figures 7E and 7F) and examined their photoabsorption in vitro (Figures 7G and 7H). As expected, GUR-3 showed little absorption of UVB light (Figure 7H). By contrast, strong absorption of UVB light at 280 nm was observed in GUR-3^{Y79W} (Figure 7G). The extinction coefficient of this tryptophan-bearing GUR-3^{Y79W} protein reached the level of 10^6 $M^{-1}cm^{-1}$ (1.03×10^6 $M^{-1}cm^{-1}$), which is about one-third of that found for LITE-1. This data provides a biochemical basis for the observed photosensitivity of GUR-3^{Y79W}. This set of experiments also raises the intriguing prospect that it might be possible to genetically engineer new photoreceptors.

DISCUSSION

In summary, our results demonstrate that the *C. elegans* taste receptor homolog LITE-1 is a bona fide photoreceptor. As some photoreceptors are multifunctional—for example, *Drosophila* rhodopsin also responds to heat (Shen et al., 2011)—it remains

possible that LITE-1 might also be able to sense additional cues, including chemical cues such as H_2O_2 (Bhatla and Horvitz, 2015). Several features distinguish LITE-1 from known photoreceptors, including an exceptionally high efficiency in photoabsorption, an ability to sense both UVA and UVB light, a strict dependence on protein conformation for photoabsorption, a strong resistance to photobleaching, and a reversed membrane topology compared to opsins. LITE-1 also bears no sequence homology with the two known metazoan photoreceptors (i.e., opsins and cryptochromes) or any other photoreceptors in microbes and plants. Apparently, LITE-1 represents a distinct type of photoreceptor in nature.

While it is easy to appreciate the requirement of tryptophan residues for the absorption of UVB light at 280 nm, it is a bit surprising that the absorption of UVA light at 320 nm also depends on the same tryptophan residues. On the other hand, some mutations (e.g., S226F and A332V) only affect the absorption of UVA but not UVB light (Figures 5A and 5B). As such, we suggest that the two tryptophan residues W77 and W328 regulate the absorption of both UVB and UVA light, while the absorption of UVA light requires additional residues such as S226 and A332. The W77F and W328F data, together with the unusually strict dependence of LITE-1 photoabsorption on its protein conformation, raise the intriguing possibility that LITE-1 may not have a prosthetic chromophore. Interestingly, the plant-specific protein UVR8, a soluble protein that is completely unrelated to LITE-1, also requires tryptophan residues for UVB light detection and lacks a prosthetic chromophore (Christie et al., 2012; Rizzini et al., 2011; Wu et al., 2012). This prompted us to speculate that the two tryptophan residues W77 and W328 may contribute to the formation of the chromophore of LITE-1, which may underlie its high photon-capturing efficiency. Though the definitive answer shall await the determination of the atomic structure of LITE-1, our finding that introducing such a tryptophan residue into another GR family protein can promote photosensitivity lends support to this model. This experiment also raises the intriguing prospect that it might be possible to genetically engineer new photoreceptors.

LITE-1 is a member of the invertebrate GR gene family, which contains five homologs in worms and more than 60 members in insects (Clyne et al., 2000; Liu et al., 2010; Scott et al., 2001). Some of them in fact do not act as chemoreceptors (Thorne and Amrein, 2008). For example, *Drosophila* Gr28b(d) encodes a thermosensor (Ni et al., 2013), while another Gr28b isoform has been implicated in UV-light-induced avoidance behavior (Xiang et al., 2010). The inverted membrane topology makes it unlikely for LITE-1 to function as a GPCR. Interestingly, LITE-1 can functionally interact with G protein signaling (Liu et al., 2010); but given the atypical topology of LITE-1, its interaction with G protein signaling is likely to be indirect (Liu et al., 2010). It is also unclear whether LITE-1 possesses ion channel activity like some OR and GR members. At the sequence level, no clear mammalian LITE-1 homologs could be identified. This, however, does not necessarily imply a lack of LITE-1 orthologs in mammals, as 7-TM receptors tend to share limited homologies even among those within the same subfamilies. In fact, 7-TM receptors with a reversed membrane topology are present in the mammalian genome (Iwabu et al., 2010). For example, the 7-TM adiponectin receptors AdipR1 and AdipR2, which play a pivotal role in diabetes, obesity, and insulin resistance in mammals, also bear a membrane topology opposite to classical GPCRs (Iwabu et al., 2010). Some mammalian tissues/cells (e.g., skin keratinocytes and melanocytes) are sensitive to UV light, but the underlying photoreceptors have not been definitively identified (Bellono et al., 2013; Moore et al., 2013). It is conceivable that some receptor proteins functionally related to LITE-1 may sense UV light in these skin cells.

Ectopic expression of LITE-1 can confer photosensitivity to photo-insensitive cells by triggering neuronal excitation and muscle contraction (Edwards et al., 2008; Liu et al., 2010). LITE-1's exceptionally high efficiency in photon absorption, sensitivity to both UVA and UVB light, and strong resistance to photobleaching make it a promising candidate as an optogenetic tool. These features also demonstrate the potential for developing LITE-1 as an organic additive to sunscreens for skin protection against harmful UV in the sunlight. The current study provides an entry point to characterize this interesting photoreceptor.

STAR★METHODS

Detailed methods are provided in the online version of this paper and include the following:

- KEY RESOURCES TABLE
- CONTACT FOR REAGENT AND RESOURCE SHARING
- EXPERIMENTAL MODEL AND SUBJECT DETAILS
- METHODS DETAILS
  - Immunostaining to determine the membrane topology of LITE-1
  - Purification and spectrophotometric analysis of LITE-1 and control proteins
  - Behavior assays to quantify LITE-1 function
  - Calcium imaging to quantify LITE-1 function
  - Molecular biology
- QUANTIFICATION AND STATISTICAL ANALYSIS

SUPPLEMENTAL INFORMATION

Supplemental Information includes seven figures and two movies and can be found with this article online at http://dx.doi.org/10.1016/j.cell.2016.10.053.

AUTHOR CONTRIBUTIONS

J.G. performed the experiments and analyzed the data. Y.Y., B.Z., Z.W., J.P., and Z.F. assisted J.G. in performing the experiments. A.W. initiated the project and generated reagents. L.K. performed immunostaining on primary cultured muscle cells and analyzed the data. J.G., J.L., and X.Z.S.X. wrote the paper.

ACKNOWLEDGMENTS

We thank Tom Kerppola for BiFC plasmids; David Salom and Kris Palczewski for technical assistance and providing strains; Zhaohui Xu for helpful discussions; and Wenyuang Zhang, Jiejun Zhou, John Tesmer, Frederick Stull, and James Bardwell for technical assistance. Some strains were obtained from the CGC. This work utilized the Core Center for Vision Research funded by P30 EY007003 from the NEI. A.W. was supported by a predoctoral training grant from the NEI (T32EY013934). This work was supported by the NSFC (31130028, 31225011, and 31420103909 to J.L.), the Program of Introducing

Talents of Discipline to Universities from the Ministry of Education of China (B08029 to J.L.), Program for Changjiang Scholars and Innovative Research Team in University (PCSIRT: IRT13016), and grants from the NIGMS (GM083241) and NEI (EY022315).

Received: December 20, 2015
Revised: September 5, 2016
Accepted: October 28, 2016
Published: November 17, 2016

REFERENCES

Bellono, N.W., Kammel, L.G., Zimmerman, A.L., and Oancea, E. (2013). UV light phototransduction activates transient receptor potential A1 ion channels in human melanocytes. Proc. Natl. Acad. Sci. USA *110*, 2383–2388.

Benton, R., Sachse, S., Michnick, S.W., and Vosshall, L.B. (2006). Atypical membrane topology and heteromeric function of Drosophila odorant receptors in vivo. PLoS Biol. *4*, e20.

Bhatla, N., and Horvitz, H.R. (2015). Light and hydrogen peroxide inhibit C. elegans Feeding through gustatory receptor orthologs and pharyngeal neurons. Neuron *85*, 804–818.

Christensen, M., Estevez, A., Yin, X., Fox, R., Morrison, R., McDonnell, M., Gleason, C., Miller, D.M., 3rd, and Strange, K. (2002). A primary culture system for functional analysis of C. elegans neurons and muscle cells. Neuron *33*, 503–514.

Christie, J.M., Arvai, A.S., Baxter, K.J., Heilmann, M., Pratt, A.J., O'Hara, A., Kelly, S.M., Hothorn, M., Smith, B.O., Hitomi, K., et al. (2012). Plant UVR8 photoreceptor senses UV-B by tryptophan-mediated disruption of cross-dimer salt bridges. Science *335*, 1492–1496.

Clyne, P.J., Warr, C.G., and Carlson, J.R. (2000). Candidate taste receptors in Drosophila. Science *287*, 1830–1834.

de Bono, M., and Maricq, A.V. (2005). Neuronal substrates of complex behaviors in C. elegans. Annu. Rev. Neurosci. *28*, 451–501.

Dutta, A., Kim, T.Y., Moeller, M., Wu, J., Alexiev, U., and Klein-Seetharaman, J. (2010). Characterization of membrane protein non-native states. 2. The SDS-unfolded states of rhodopsin. Biochemistry *49*, 6329–6340.

Edwards, S.L., Charlie, N.K., Milfort, M.C., Brown, B.S., Gravlin, C.N., Knecht, J.E., and Miller, K.G. (2008). A novel molecular solution for ultraviolet light detection in Caenorhabditis elegans. PLoS Biol. *6*, e198.

Falciatore, A., and Bowler, C. (2005). The evolution and function of blue and red light photoreceptors. Curr. Top. Dev. Biol. *68*, 317–350.

Foster, R.G., and Soni, B.G. (1998). Extraretinal photoreceptors and their regulation of temporal physiology. Rev. Reprod. *3*, 145–150.

Fridovich, I. (2013). Oxygen: how do we stand it? Med. Princ. Pract. *22*, 131–137.

Hagins, F.M. (1973). Purification and partial characterization of the protein component of squid rhodopsin. J. Biol. Chem. *248*, 3298–3304.

Hu, C.D., Chinenov, Y., and Kerppola, T.K. (2002). Visualization of interactions among bZIP and Rel family proteins in living cells using bimolecular fluorescence complementation. Mol. Cell *9*, 789–798.

Hubbard, R. (1969). Absorption spectrum of rhodopsin: 500 nm absorption band. Nature *221*, 432–435.

Insinna, C., Daniele, L.L., Davis, J.A., Larsen, D.D., Kuemmel, C., Wang, J., Nikonov, S.S., Knox, B.E., and Pugh, E.N., Jr. (2012). An S-opsin knock-in mouse (F81Y) reveals a role for the native ligand 11-cis-retinal in cone opsin biosynthesis. J. Neurosci. *32*, 8094–8104.

Iwabu, M., Yamauchi, T., Okada-Iwabu, M., Sato, K., Nakagawa, T., Funata, M., Yamaguchi, M., Namiki, S., Nakayama, R., Tabata, M., et al. (2010). Adiponectin and AdipoR1 regulate PGC-1alpha and mitochondria by Ca(2+) and AMPK/SIRT1. Nature *464*, 1313–1319.

Kolesnikov, A.V., Kisselev, O.G., and Kefalov, V.J. (2014). Signaling by Rod and Cone Photoreceptors: Opsin Properties, G-protein Assembly, and Mechanisms of Activation. In G Protein Signaling Mechanisms in the Retina, K.A. Martemyanov and A.P. Sampath, eds. (Springer).

Li, Z., Liu, J., Zheng, M., and Xu, X.Z. (2014). Encoding of both analog- and digital-like behavioral outputs by one C. elegans interneuron. Cell *159*, 751–765.

Liu, J., Ward, A., Gao, J., Dong, Y., Nishio, N., Inada, H., Kang, L., Yu, Y., Ma, D., Xu, T., et al. (2010). C. elegans phototransduction requires a G protein-dependent cGMP pathway and a taste receptor homolog. Nat. Neurosci. *13*, 715–722.

Liu, J., Zhang, B., Lei, H., Feng, Z., Liu, J., Hsu, A.L., and Xu, X.Z. (2013). Functional aging in the nervous system contributes to age-dependent motor activity decline in C. elegans. Cell Metab. *18*, 392–402.

Maglova, L., Atanasov, B., and Keszthelyi, L. (1989). Unfolding of monomeric bacteriorhodopsin in water-urea solution. Biochim. Biophys. Acta *975*, 271–276.

Marti, T., Rösselet, S.J., Otto, H., Heyn, M.P., and Khorana, H.G. (1991). The retinylidene Schiff base counterion in bacteriorhodopsin. J. Biol. Chem. *266*, 18674–18683.

Matsuyama, T., Yamashita, T., Imamoto, Y., and Shichida, Y. (2012). Photochemical properties of mammalian melanopsin. Biochemistry *51*, 5454–5462.

Moore, C., Cevikbas, F., Pasolli, H.A., Chen, Y., Kong, W., Kempkes, C., Parekh, P., Lee, S.H., Kontchou, N.A., Yeh, I., et al. (2013). UVB radiation generates sunburn pain and affects skin by activating epidermal TRPV4 ion channels and triggering endothelin-1 signaling. Proc. Natl. Acad. Sci. USA *110*, E3225–E3234.

Ni, L., Bronk, P., Chang, E.C., Lowell, A.M., Flam, J.O., Panzano, V.C., Theobald, D.L., Griffith, L.C., and Garrity, P.A. (2013). A gustatory receptor paralogue controls rapid warmth avoidance in Drosophila. Nature *500*, 580–584.

Oesterhelt, D., and Hess, B. (1973). Reversible photolysis of the purple complex in the purple membrane of Halobacterium halobium. Eur. J. Biochem. *37*, 316–326.

Okano, T., Fukada, Y., Shichida, Y., and Yoshizawa, T. (1992). Photosensitivities of iodopsin and rhodopsins. Photochem. Photobiol. *56*, 995–1001.

Radding, C.M., and Wald, G. (1956). Acid-base properties of rhodopsin and opsin. J. Gen. Physiol. *39*, 909–922.

Rizzini, L., Favory, J.J., Cloix, C., Faggionato, D., O'Hara, A., Kaiserli, E., Baumeister, R., Schäfer, E., Nagy, F., Jenkins, G.I., and Ulm, R. (2011). Perception of UV-B by the Arabidopsis UVR8 protein. Science *332*, 103–106.

Salom, D., Cao, P., Sun, W., Kramp, K., Jastrzebska, B., Jin, H., Feng, Z., and Palczewski, K. (2012). Heterologous expression of functional G-protein-coupled receptors in Caenorhabditis elegans. FASEB J. *26*, 492–502.

Scott, K., Brady, R., Jr., Cravchik, A., Morozov, P., Rzhetsky, A., Zuker, C., and Axel, R. (2001). A chemosensory gene family encoding candidate gustatory and olfactory receptors in Drosophila. Cell *104*, 661–673.

Shen, W.L., Kwon, Y., Adegbola, A.A., Luo, J., Chess, A., and Montell, C. (2011). Function of rhodopsin in temperature discrimination in Drosophila. Science *331*, 1333–1336.

Sperling, W., and Rafferty, C.N. (1969). Relationship between absorption spectrum and molecular conformations of 11-cis-retinal. Nature *224*, 590–594.

Thompson, C.L., and Sancar, A. (2002). Photolyase/cryptochrome blue-light photoreceptors use photon energy to repair DNA and reset the circadian clock. Oncogene *21*, 9043–9056.

Thorne, N., and Amrein, H. (2008). Atypical expression of Drosophila gustatory receptor genes in sensory and central neurons. J. Comp. Neurol. *506*, 548–568.

Vought, B.W., Dukkipatti, A., Max, M., Knox, B.E., and Birge, R.R. (1999). Photochemistry of the primary event in short-wavelength visual opsins at low temperature. Biochemistry *38*, 11287–11297.

Wang, T., and Montell, C. (2007). Phototransduction and retinal degeneration in Drosophila. Pflugers Arch. *454*, 821–847.

Wang, R., Mellem, J.E., Jensen, M., Brockie, P.J., Walker, C.S., Hoerndli, F.J., Hauth, L., Madsen, D.M., and Maricq, A.V. (2012). The SOL-2/Neto auxiliary

protein modulates the function of AMPA-subtype ionotropic glutamate receptors. Neuron *75*, 838–850.

Ward, A., Liu, J., Feng, Z., and Xu, X.Z. (2008). Light-sensitive neurons and channels mediate phototaxis in C. elegans. Nat. Neurosci. *11*, 916–922.

Wu, L.Z., Sheng, Y.B., Xie, J.B., and Wang, W. (2008). Photoexcitation of tryptophan groups induced reduction of disulfide bonds in hen egg white lysozyme. J. Mol. Struct. *882*, 101–106.

Wu, D., Hu, Q., Yan, Z., Chen, W., Yan, C., Huang, X., Zhang, J., Yang, P., Deng, H., Wang, J., et al. (2012). Structural basis of ultraviolet-B perception by UVR8. Nature *484*, 214–219.

Xiang, Y., Yuan, Q., Vogt, N., Looger, L.L., Jan, L.Y., and Jan, Y.N. (2010). Light-avoidance-mediating photoreceptors tile the Drosophila larval body wall. Nature *468*, 921–926.

Xiao, R., Zhang, B., Dong, Y., Gong, J., Xu, T., Liu, J., and Xu, X.Z.S. (2013). A genetic program promotes C. elegans longevity at cold temperatures via a thermosensitive TRP channel. Cell *152*, 806–817.

Yau, K.W., and Hardie, R.C. (2009). Phototransduction motifs and variations. Cell *139*, 246–264.

Zhang, H.J., Anderson, A.R., Trowell, S.C., Luo, A.R., Xiang, Z.H., and Xia, Q.Y. (2011). Topological and functional characterization of an insect gustatory receptor. PLoS ONE *6*, e24111.

STAR★METHODS

KEY RESOURCES TABLE

REAGENT or RESOURCE	SOURCE	IDENTIFIER
Antibodies		
Mouse monoclonal anti-1D4	Polgenix	N/A
Rabbit monoclonal anti-C-LITE-1	This paper	N/A
Rabbit monoclonal anti-N-LITE-1	This paper	N/A
Mouse monoclonal anti-N-Myc	ThermoFisher	CAT# MA1-16638; RRID: AB_2235735
Chemicals, Peptides, and Recombinant Proteins		
bis-trsi-propane	Sigma	CAT# 79-97-0
proteinase inhibitor cocktail	Roche	CAT# 11836170001
n-dodecyl-β-D-maltopyranoside	Affymentrix	CAT# 69227-93-6
9-cis-retinal	Toronto Research Chemicals	CAT# 514-85-2
Hydrogen peroxide solution	Sigma	CAT# 7722-84-1
Urea	Sigma	CAT# 57-31-6
1D4 peptide	Genscript	Lot# 89521380001
Critical Commercial Assays		
Bradford protein assay	Bio-Rad	CAT# 5000001
ECL western blotting kit	ThermoFisher	CAT# 35050
Experimental Models: Organisms/Strains		
C. elegans: lite-1(xu7)	Ward et al., 2008; Caenorhabditis Genetics Center	TQ800
C. elegans: N2	Caenorhabditis Genetics Center	WormBase: N2
C. elegans: xuIs98 [Pmyo-3::lite-1::1D4::SL2::YFP]	This paper	TQ2518
C. elegans: xuIs397 [Pmyo-3::lite-1(W328F)::1D4::SL2::YFP]	This paper	TQ6448
C. elegans: xuIs399 [Pmyo-3::lite-1(W77F)::1D4::SL2::YFP]	This paper	TQ6450
C. elegans: xuIs403 [Pmyo-3::lite-1(A332V)::1D4::SL2::YFP]	This paper	TQ6454
C. elegans: xuIs404 [Pmyo-3::lite-1(S226F)::1D4::SL2::YFP]	This paper	TQ6455
C. elegans: xuEx1623 [Pmyo-3::lite-1(W77A)::1D4::SL2::YFP]	This paper	TQ5143
C. elegans: xuEx1627 [Pmyo-3::lite-1(W191A)::1D4::SL2::YFP]	This paper	TQ5148
C. elegans: xuEx1628 [Pmyo-3::lite-1(W319A)::1D4::SL2::YFP]	This paper	TQ5149
C. elegans: xuEx1629 [Pmyo-3::lite-1(W328A)::1D4::SL2::YFP]	This paper	TQ5150
C. elegans: xuEx1632 [Pmyo-3::lite-1(W41A)::1D4::SL2::YFP]	This paper	TQ5152
C. elegans: xuEx1633 [Pmyo-3::lite-1(W419A)::1D4::SL2::YFP]	This paper	TQ5153
C. elegans: xuEx2430[Pmyo-3::bJun::N-YFP::lite-1::SL2::DsRed]	This paper	TQ6688
C. elegans: xuEx2431[Pmyo-3::bFos::C-YFP]	This paper	TQ6689
C. elegans: xuEx2432[Pmyo-3:: ΔbFos::C-YFP]	This paper	TQ6690
C. elegans: xuEx386[Pmyo-3::myc::lite-1::SL2::YFP]	This paper	TQ1353
C. elegans: xuIs32[Pmyo-3::lite-1::SL2::YFP]	This paper	TQ1230
C. elegans: xuIs442[Pmyo-3::GUR-3(Y79W)::1D4::SL2::YFP]	This paper	TQ7405
C. elegans: xuIs441[Pmyo-3::GUR-3::1D4::SL2::YFP]	This paper	TQ7404
C. elegans: xuIs444[Pmyo-3::RCaMP]; lite-1(xu7)	This paper	TQ7428
Recombinant DNA		
Pmyo-3::lite-1::1D4::SL2::YFP	This paper	pSX1580
Pmyo-3::lite-1(W328F)::1D4::SL2::YFP	This paper	pSX1712
Pmyo-3::lite-1(W77F)::1D4::SL2::YFP	This paper	pSX1713
Pmyo-3::lite-1(A332V)::1D4::SL2::YFP	This paper	pSX1710

(*Continued on next page*)

Continued

REAGENT or RESOURCE	SOURCE	IDENTIFIER
Pmyo-3::lite-1(S226F)::1D4::SL2::YFP	This paper	pSX1711
Pmyo-3::lite-1(W77A)::1D4::SL2::YFP	This paper	pSX1714
Pmyo-3::lite-1(W191A)::1D4::SL2::YFP	This paper	pSX1715
Pmyo-3::lite-1(W319A)::1D4::SL2::YFP	This paper	pSX1716
Pmyo-3::lite-1(W328A)::1D4::SL2::YFP	This paper	pSX1717
Pmyo-3::lite-1(W41A)::1D4::SL2::YFP	This paper	pSX1718
Pmyo-3::lite-1(W419A)::1D4::SL2::YFP	This paper	pSX1719
Pmyo-3::bJun::N-YFP::lite-1::SL2::DsRed	This paper	pSX1740
Pmyo-3::bFos::C-YFP	This paper	pSX1741
Pmyo-3:: ΔbFos::C-YFP	This paper	pSX1742
Pmyo-3::myc::lite-1::SL2::YFP	This paper	pSX153
Pmyo-3::GUR-3(Y79W)::1D4::SL2::YFP	This paper	pSX1902
Pmyo-3::GUR-3::1D4::SL2::YFP	This paper	pSX1903
Pmyo-3::RCaMP	This paper	pSX1904
Software and Algorithms		
Wormlab system	MBF Bioscience	N/A
MetaFluor	Molecular Devices	N/A

CONTACT FOR REAGENT AND RESOURCE SHARING

Requests for reagents and resources may be directed to the Lead Contact, X.Z. Shawn Xu (shawnxu@umich.edu).

EXPERIMENTAL MODEL AND SUBJECT DETAILS

C. elegans strains were maintained at 20°C on nematode growth medium (NGM) plates seeded with OP50 bacteria. Liquid culture was used to produce large quantities of worms for protein purification (see Methods Details). Transgenic lines were generated by injecting plasmid DNA directly into hermaphrodite gonad. Integrated transgenic strains were outcrossed at least six times before used for protein purification.

METHODS DETAILS

Immunostaining to determine the membrane topology of LITE-1

Immunostaining was performed on primary cultured cells using standard protocols (Christensen et al., 2002). Muscle cells co-expressed LITE-1 and GFP or expressed GFP alone as a transgene driven by the muscle-specific promoter *myo-3*. Gravid hermaphrodites were lysed to release eggs, and embryos were dissociated by chitinase treatment and trituration, filtered through a 5 μm membrane, plated on cover glasses coated with peanut lectin, and cultured in L15 with 10% serum (340-345 mOsm) at 20°C. To perform non-permeablized surface staining, live cells were first blocked with 3% BSA and 5% normal goat serum (NGS) in PBS for 30 min, and then incubated with primary antibodies (1 μg/ml) for one hour in PBS (1.5% BSA) at room temperature. Following three washes with PBS, cells were fixed for 10 min with 1.5% paraformaldehyde (PFA) in PBS followed by three washes with PBS and one hour incubation in second antibodies (1:2000, Cy3 conjugated). After five washes with PBS, cover glasses were mounted for imaging analysis. To perform permeabilized staining, cells were first fixed with 1.5% PFA in PBS for 10 min at room temperature, rinsed three times with PBS, and permeabilized with 0.5% Trition X-100 in PBS for 5 min. After three washes with PBS, cells were blocked with BSA and NGS, incubated with primary antibodies, and washed five times. Following one hour incubation with secondary antibodies, cover glasses were rinsed five times before mounting. The N- and C-terminal end peptides (15 residues) were used to immunize rabbits to generate LITE-1 antibodies which were affinity-purified before use for staining (YenZym Antibodies).

Purification and spectrophotometric analysis of LITE-1 and control proteins

Worms were cultured in the dark. They were first cultured on NGM plates and then transferred to 10 liters of S medium for liquid culture using a fermenter (New Brunswick, 20°C, 50% dissolved oxygen, 300 rpm agitation, pH7.2) with the support from concentrated HB101 bacteria. After 2 generations (about 7-8 days) in the fermenter, worms were harvested and suspended in 80 mL of 25 mM *bis-trsi*-propane (BTP) buffer (pH7.2) supplemented with proteinase inhibitor cocktail (Complete Mini, EDTA-free). All purification steps were carried out in the dark. A microfluidizer (Microfluidics) was used to break the worms (120 psi, 5 cycles). After removing the debris

by low speed centrifugation at 1,000 g for 10 min at 4°C, the supernatant was collected and centrifuged again at high speed (100,000 g) for 1 hr at 4°C to pellet cell membranes, which were solubilized with 20 mM *n*-dodecyl-β-D-maltopyranoside (DDM; Affymentrix) in BTP buffer (pH7.2) containing 500mM NaCl. After removing unsolubilized materials by centrifugation at 40,000 g for 30 min, we loaded the extract to an α1D4 affinity column. Note: we attached a 1D4 tag to the C terminus of LITE-1 and GUR-3 expressed as a transgene in the worm muscle, as described for A_{2A} receptor (Salom et al., 2012). Bovine rhodopsin (Rho) has this tag sequence at its C terminus. After washing with the washing buffer (10 mM DDM in 25 mM BTP buffer [pH7.2] and 500mM NaCl), we eluded LITE-1 with 1.5 mg/ml of 1D4 peptide diluted in this buffer. Purified LITE-1 was loaded onto a molecular size separation column (GE healthcare Bio-Sciences) to remove 1D4 peptide before spectrophotometric analysis. When purifying bovine rhodopsin (Rho), 2 mM 9-cis-retinal was used to resuspend pelleted cell membranes and incubate for 30 min prior to solubilization with DDM. This treatment was not performed when purifying LITE-1, GUR-3, or A_{2A} receptor. Purified protein samples used for SDS-PAGE were prepared under non-reducing conditions at room temperature (no heating) to avoid aggregation.

The concentration of purified proteins was first determined by the Bradford assay (Bio-Rad), and then verified by SDS-PAGE followed by Coomassie staining using rhodopsin as a standard. The concentration data were also independently verified by silver staining following SDS-PAGE using rhodopsin as a standard.

Spectrophotometric analysis was performed on a UV-Vis spectrophotometer (Varian Cary 50) in a quartz cuvette. Samples and reference blanks were all diluted in the same washing buffer. Note: 1D4 peptide was removed from samples prior to spectrophotometric analysis (see above). For those experiments involving treatment with denaturing agents or H_2O_2, LITE-1 was incubated with these agents for 5 min at room temperature prior to spectrophotometric analysis. All the assays were carried out in the dark.

Behavior assays to quantify LITE-1 function

Body paralysis assay was performed on day 1 gravid adult hermaphrodites, which were raised on NGM plates, under a Zeiss fluorescence dissection scope (Zeiss Discovery) coupled with an M2Bio lens system from Kramer Scientifics. The assay was done on NGM plates without OP50 using a protocol similar to that for assaying phototaxis behavior (Liu et al., 2010; Ward et al., 2008). UVA light pulses (350 ± 20 nm, 0.8 mW/mm^2, up to 20 s) were delivered from an Arc lamp (X-Cite 120) to the worm through a 10x lens in combination with 2.5x zoom. To deliver UVB light, we attached a 280 ± 10 nm excitation filter (from Semrock, 0.03 mW/mm2) to the end of the liquid light guide of the lamp, which was then directly pointed to the worm using a micromanipulator. We manually moved the dish to keep the worm in the view field. In another assay, we quantified body paralysis by monitoring locomotion speed decrease over time using the Wormlab system (MBF Bioscience). UVA and UVB light was directed to the worm using a liquid light guide as described above. To minimize the effect of endogenous *lite-1* gene on locomotion speed under UV light (Liu et al., 2010), this assay was performed in *lite-1(xu7)* mutant background for all genotypes. A total of 20-50 animals were assayed for each genotype in each experiment unless otherwise indicated. The sample size of each assay was found to be adequate after running power analysis ($p > 0.8$). Each worm was assayed five times, and once the worm was paralyzed, we stopped the assay to let it recover for next round of test.

Calcium imaging to quantify LITE-1 function

Calcium imaging of muscle cells was performed on an inverted microscope (Olympus IX73) under a 60x lens as previously described (Li et al., 2014; Xiao et al., 2013). RCaMP was expressed as a transgene in muscle cells using the *myo-3* promoter. Transgenic worms expressing LITE-1 or control worms were glued on an agarose pad and bathed in solution (10 mM HEPES [pH 7.4], 5 mM KCl, 145 mM NaCl,1.2 mM $MgCl_2$, 2.5 mM $CaC1_2$, and 10 mM glucose). UV light (UVA: 340 ± 20 nm, 0.7 mW/mm^2; UVB: 280 ± 10 nm, 0.02 mW/mm2; 5 s) was directly projected to the worm through a liquid light guide mounted on a micromanipulator. Images were acquired under yellow light (575 ± 25 nm) with a Roper CoolSnap CCD camera and processed with MetaFluor software (Molecular Devices). To minimize the contribution from endogenous photosensation system, all genotypes, including WT, carried *lite-1(xu7)* mutation in the background (Liu et al., 2010). The peak percentage change in the intensity of RCaMP fluorescence (ΔF/F) was quantified.

Molecular biology

All the plasmids are listed in the Key Resources Table. All the LITE-1 and GUR-3 constructs carry a 1D4 tag at the C terminus, with the exception in Figure 1 where no such a tag was included to LITE-1. Myc tag was only included in the construct used in Figure 1B. As listed in the Key Resources Table, some plasmids contain an SL2::YFP fragment, which directs expression of YFP as a separate transcript under the control of the same promoter of its upstream gene in an operon-like fashion. This enables expression of YFP as a co-expression marker in muscle cells under the control of the same muscle-specific *myo-3* promoter that drives expression of LITE-1.

QUANTIFICATION AND STATISTICAL ANALYSIS

Quantification and statistical parameters were indicated in the legends of each figure, including error bars (SEM), n numbers, and p values. For those involving multiple group comparisons, we applied ANOVA followed by a post hoc test. We considered p values of < 0.05 significant.

Cell

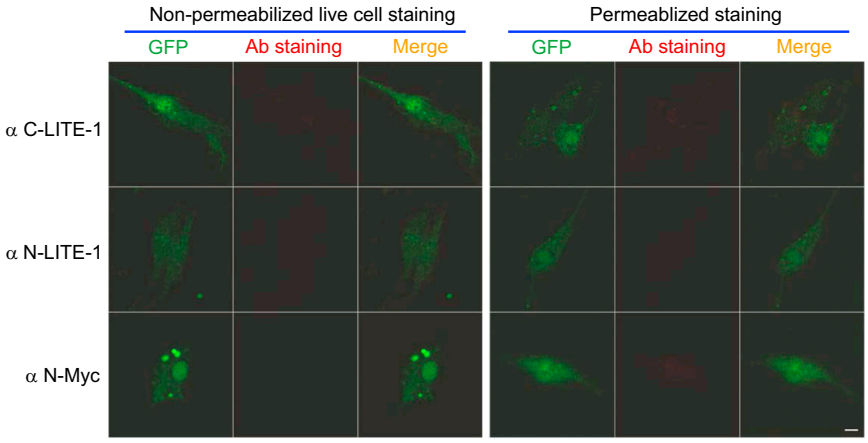

Figure S1. Control Images for Figure 1B, Related to Figure 1

Immunostaining was conducted as described in Figure 1B. Primary cultured cells were derived from transgenic worms expressing GFP only but not LITE-1 in muscle cells under the *myo-3* promoter. No LITE-1 signal was detected, showing that LITE-1 staining seen in Figure 1B is specific.

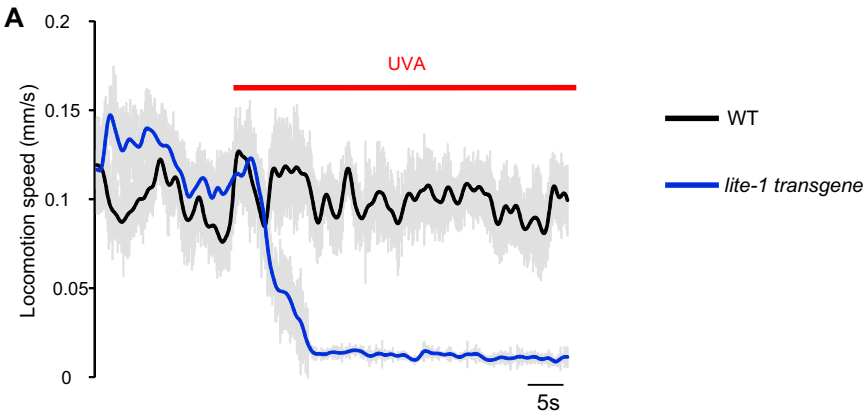

Figure S2. Ectopic Expression of LITE-1 as a Transgene in Muscle Cells Confers Photosensitivity, Related to Figure 2

LITE-1 was expressed as a transgene in muscle cells under the *myo-3* promoter. Worm locomotion speed was monitored and quantified by WormLab system (MBF Bioscience). UVA light (350 ± 20 nm, 0.8 mW/mm2) was directed to worms, which induced muscle contraction in *lite-1* transgenic worms but not in WT worms, leading to the paralysis of the former (locomotion speed reduced to zero), but not the latter. To minimize the effect of endogenous *lite-1* gene on locomotion speed under UV light, the experiments were done in *lite-1(xu7)* mutant background (i.e., both genotypes carried *lite-1(xu7)* mutation). Shades along the traces denote error bars (SEM). n = 25.

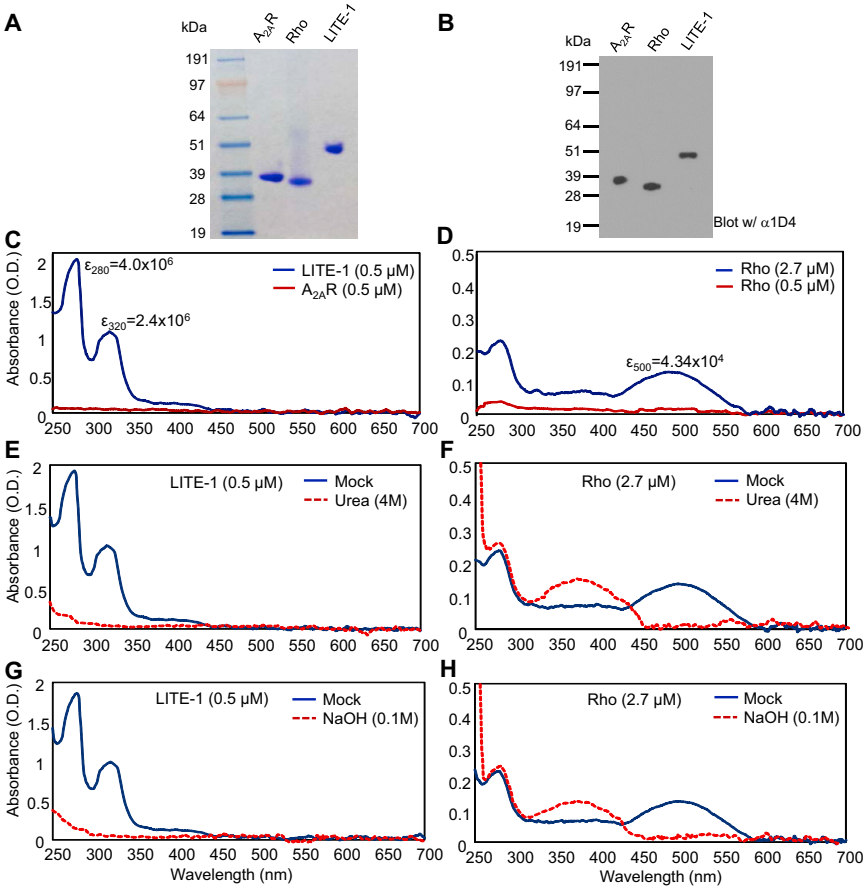

Figure S3. Comparison of the Spectral Properties of LITE-1, Bovine Rhodopsin, and Adenosine A_{2A} Receptor Purified from Worm Muscles, Related to Figure 2

(A and B) LITE-1, Rho, and $A_{2A}R$ were purified side-by-side from transgenic worms under the same conditions. All transgenes have a 1D4 tag at the C terminus. (A) Coomassie staining. (B) Western.

(C) LITE-1 shows strong photoabsorption at 0.5 μM, whereas $A_{2A}R$ does not.

(D) Rho shows minimal photoabsorption at 0.5 μM, and only shows modest photoabsorption at a higher concentration (2.7 μM). Note: the y axis scale in (C) and (D) are different.

(E and F) Denaturing LITE-1 with urea abolishes its photoabsorption (E), whereas the same treatment does not eliminate the photoabsorption of Rho and instead shifts its 500 nm absorbance peak to 370 nm (F).

(G and H) Denaturing LITE-1 with NaOH abolishes its photoabsorption (E), whereas the same treatment on Rho does not and instead shifts its 500 nm absorbance peak to 370 nm (F).

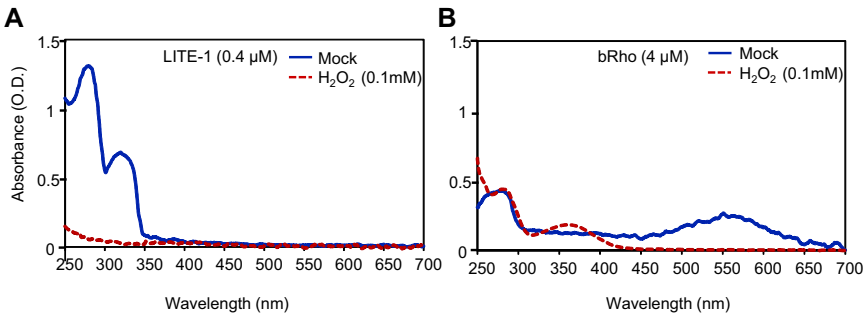

Figure S4. The Impact of H_2O_2 on LITE-1 Photoabsorption, Related to Figure 3

(A) H_2O_2 treatment abolishes the light absorption of LITE-1. LITE-1 was treated with H_2O_2 (0.1 mM) for 5 min at room temperature prior to spectral analysis. (B) H_2O_2 treatment does not abolish the photosensitivity of bacterial rhodopsin (bRho) but shifts its absorbance peak from 568 nm to 370 nm. bRho was treated with H_2O_2 (0.1 mM) for 5 min at room temperature prior to spectral analysis. A similar phenomenon was observed with purified bovine rhodopsin (not shown).

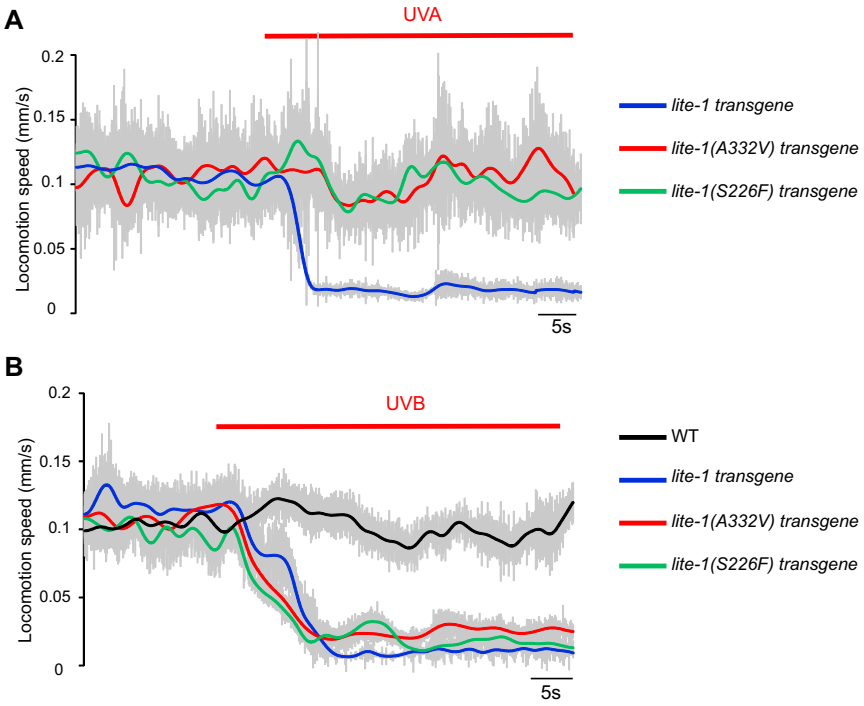

Figure S5. Residues S226 and A332 in LITE-1 Are Critical for Its Sensitivity to UVA but Not UVB Light In Vivo, Related to Figures 4 and 5

(A and B) LITE-1^{S226F} and LITE-1^{A332V} were expressed as a transgene in muscle cells under the *myo-3* promoter. Worm locomotion speed was monitored and quantified by WormLab system (MBF Bioscience). UVA (350 ± 20 nm, 0.8 mW/mm2) (A) or UVB (280 ± 10 nm, 0.03 mW/mm2) (B) light was directed to the worm, which induced muscle contraction, leading to paralysis of the worm (locomotion speed reduced to zero). To minimize the effect of endogenous *lite-1* gene on locomotion speed under UV light, the experiments were done in *lite-1(xu7)* mutant background (i.e., all genotypes carried *lite-1(xu7)* mutation). Shades along the traces denote error bars (SEM). n = 25.

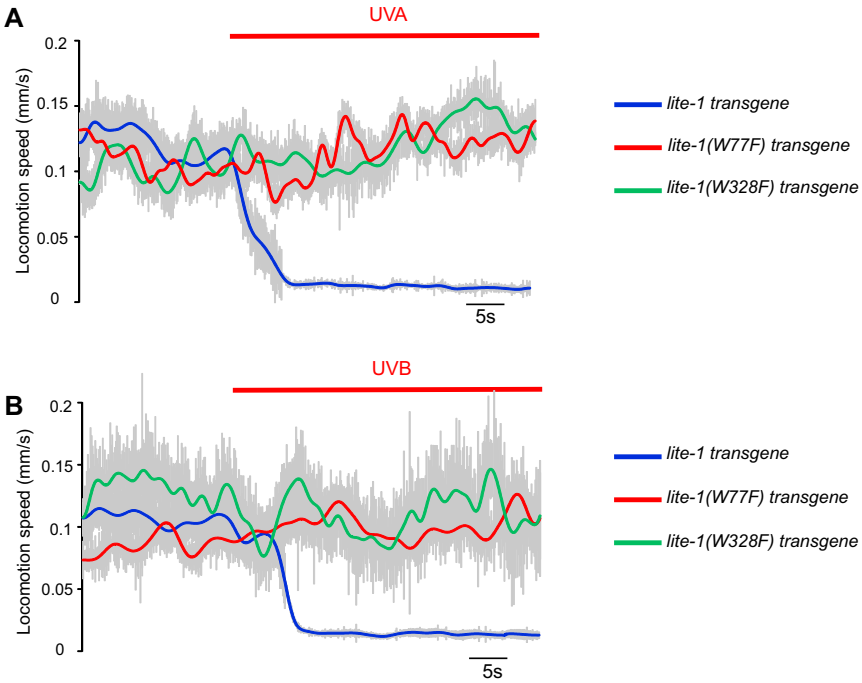

Figure S6. The Two Tryptophan Residues W77 and W328 in LITE-1 Are Required for Its Sensitivity to Both UVA and UVB Light In Vivo, Related to Figure 6

(A and B) LITE-1^{W77F} and LITE-1^{W328F} were expressed as a transgene in muscle cells under the *myo-3* promoter. Worm locomotion speed was monitored and quantified by WormLab system (MBF Bioscience). UVA (350 ± 20 nm, 0.8 mW/mm2) (A) or UVB (280 ± 10 nm, 0.03 mW/mm2) (B) light was directed to the worm. The two tryptophan mutations disrupted the ability of LITE-1 in mediating UVA- and UVB-light-induced paralysis caused by muscle contraction (locomotion speed reduced to zero). To minimize the effect of endogenous *lite-1* gene on locomotion speed under UV light, the experiments were done in *lite-1(xu7)* mutant background (i.e., all genotypes carried *lite-1(xu7)* mutation). Shades along the traces denote error bars (SEM). n = 25.

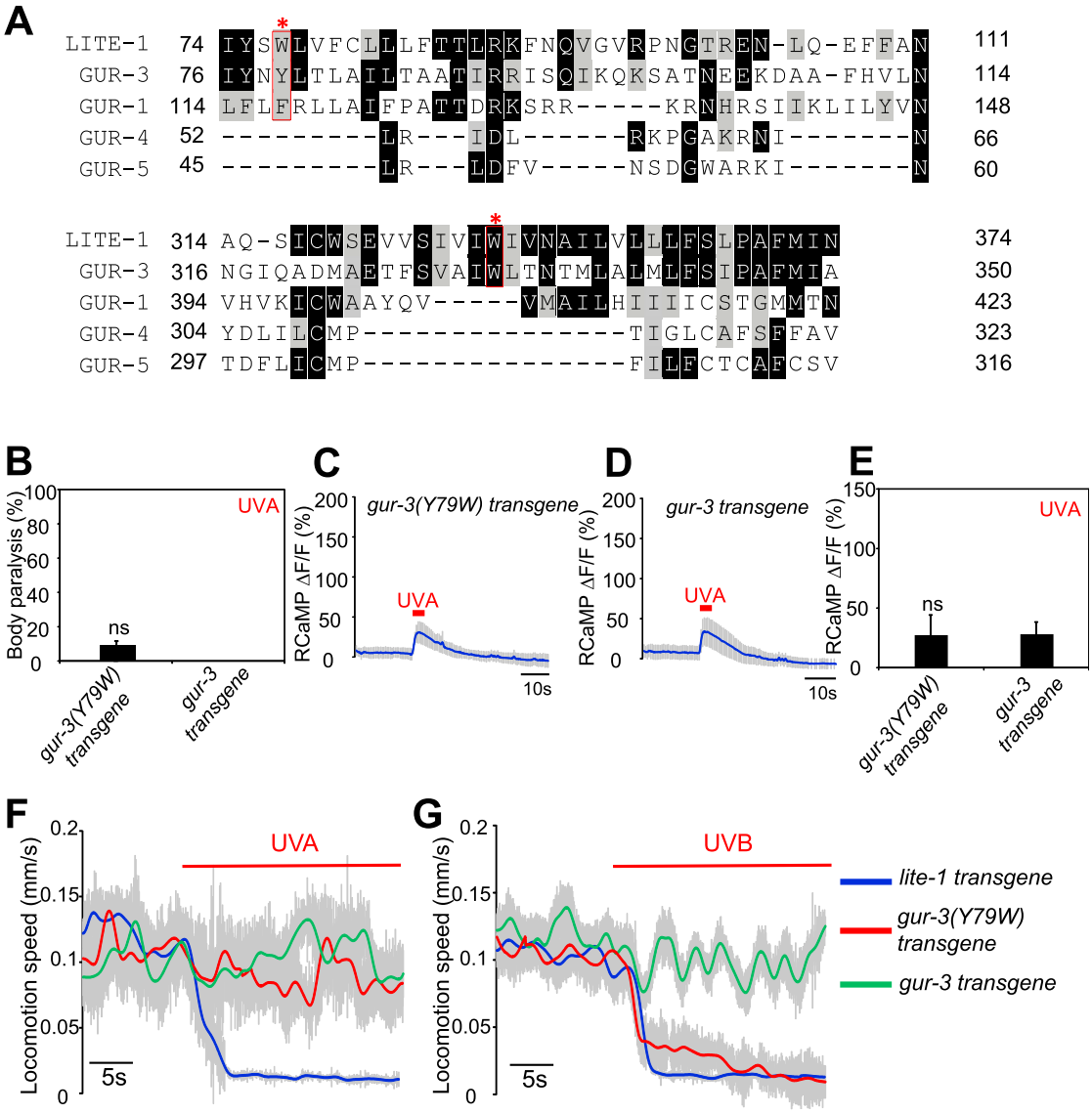

Figure S7. Sequence Alignment of *C. elegans* GR Family Proteins and Additional Data Related to GUR-3, Related to Figure 7

(A) The two tryptophan residues W77 and W328 in LITE-1 are marked with an asterisk in red. W77 is not conserved in any other GR members. W328 is only found in GUR-3. The sequences between residues 112-313 in LITE-1 are not shown, as there is limited homology in this large segment between LITE-1 and other GRs.

(B) Mutating Y79 to W in GUR-3 does not promote its sensitivity to UVA light in vivo shown by paralysis assay. GUR-3^{Y79W} and GUR-3 were expressed as a transgene in muscle cells. Worms were exposed to a 20 s pulse of UVA light (350 ± 20 nm, 0.8 mW/mm2), and those showing muscle contraction-induced paralysis during light illumination were scored positive. n = 50. Error bars: SEM p = 0.153 (t test).

(C–E) Mutating Y79 to W in GUR-3 does not promote its sensitivity to UVA light in vivo shown by calcium imaging. A 5 s pulse of UVA light (340 ± 20 nm, 0.7 mW/mm2) was directed to the worm. (C) and (D) Imaging traces. (E) Bar graph. n = 20. p = 0.779 (t test).

(F and G) Mutating Y79 to W in GUR-3 promote its sensitivity to UVB but not UVA light in vivo shown by locomotion assay. The assay was done as in Figure S6. The *lite-1* transgene traces were duplicates from Figure S6 and were included for comparison.